Changing Flood Intensities in California:

Examination of Changing Annual Peak Flow Magnitudes in the Northern Coastal Region, Sierra Nevada Mountain Region, and the Southern Coastal Region, CA.

By
Natalie Gillard
Dept. of Geography, University of Colorado at Boulder

Defended April 4, 2016

Thesis Advisor:
Dr. John Pitlick, Dept. of Geography

Defense Committee:
Dr. John Pitlick, Dept. of Geography
Dr. Holly Barnard, Dept. of Geography
Dr. Shemin Ge, Dept. of Geology

TABLE OF CONTENTS

ABSTRACT

It is widely accepted that climate change will affect precipitation patterns globally. However, studies of precipitation patterns across the United States suggest that, while the frequency of heavy precipitation events is increasing in some regions, it does not appear that flood magnitudes are increasing in any systematic way. This paper examines changes in flood intensities in three regions of California for two time periods, 1950-1981 and 1982-2014.The three regions considered are the northern coast, southern coast, and the Sierra Nevada mountain region. Changes in flood intensities are evaluated using a series of statistical tests to determine if the differences in flood magnitudes between the two time periods are statistically significant based on analyses of peak flow records from unregulated rivers in each region. The results suggest that for the majority of sites (90%) there has been no significant change in mean flood intensity between the two time periods. Two rivers in the Northern region and one in the Sierra Nevada region had significant decreases in flood magnitudes. No rivers in the Southern region have experienced significant changes in flood intensity. This is likely due to compounding factors such as variations in precipitation, soil type, vegetation, and artificial drainage networks. I conclude that few flood magnitudes are changing and in no significant spatial pattern.

KEY WORDS: Climate Change, California, Flood Magnitudes.

INTRODUCTION

It is important to understand how climate change is occurring in order to predict the changes in patterns and risks of natural hazards, such as flooding. Floods affect the human population in terms of insurance costs, infrastructure, safety and recreational/farmland use in both physical and fiscal ways. For instance, statistics provided by NOAA Hydrologic Information Center show that floods caused an average of $8.0 billion in damage per year, and 82 fatalities per year over the last 30 years (NOAA, 2014). If research can discover trends or changes in the magnitude and/or frequency of floods, mitigation plans for human safety can be developed and implemented, and human lives can be saved.

There are currently discrepancies between observed trends in “heavy” precipitation, and observed trends in flooding. Estimated changes in precipitation return value, based on daily accumulated precipitation station data, was calculated using extreme value analysis showing that 76% of all stations across the United States experienced increases in extreme precipitation with 15% showing significant increases (Kunkel, 2013). California presents increases in extreme precipitation in the central and southern regions, with a decrease in extreme precipitation in the northern region (Kunkel, 2013). Changes in precipitation do not necessarily mean changes in flooding, as large river basins are able to respond to more extreme duration precipitation events and some of the extreme events occur during periods of generally less precipitation (Peterson et al., 2013). However, it has been seen that across the United States, the southwest shows a general decrease in magnitude, whereas the north east is experiencing larger flood magnitudes (Peterson et al., 2013). California experiences atmospheric rivers that may cause extreme flooding, however, more research must be done to estimate the changes (Dettinger, 2011). Changing flood magnitude may not be the top concern, rather changes in flood frequency may have a larger affect over the United States (Mallakpour and Villarini, 2015; Hirsh and Archfield, 2015). It has been shown that there is an increase in flood frequency rather than magnitude, especially during the spring and summer months, across the central United States (Mallakpour and Villarini, 2015; Hirsh and Archfield, 2015). It would seem to be straightforward to correlate higher precipitation with higher floods, however, this has yet to be seen in analyses of flood records across most of the US (Hirsch and Archfield, 2015). Most precipitation comes from moisture already in the atmosphere at the time a storm begins (Trenberth et al., 2003). As the climate warms, the ability of the atmosphere to hold water vapor increases; therefore, models of climate change predict that rainfall will increase in intensity and decrease in duration (Trenberth et al., 2003). It is expected that flooding produced by heavy precipitation will also increase, but predictions of floods are complicated by other factors, such as the special distribution of rainfall, changes in land use and water storage.

Recent studies of patterns of precipitation and flooding across the United States suggest that trends are shifting towards heavier precipitation and increased flooding across the United States in some areas, but not in others. The distribution of flood peaks across the eastern United States shows that only a small number of stations have significant linear trends, both increasing and decreasing, and of those stations, there was no spatial structure found relating the trends (Villarini and Smith, 2010). In fact, there is little indication of human-induced climate change which relates to changing flood intensities over the eastern United States (Vallarini and Smith, 2010). In conjunction, there are significant increases in seasonal and annual water flow in the Mississippi drainage area, however, less than half of the difference can be explained by climate (Schottler et al., 2014). Additionally, models analyses of precipitation records indicate a modest level of increased precipitation in the southern and central parts of California, however, most of the trend is not significant (Mass, 2011). The present study seeks to help address that gap in research by analyzing changing flood intensities in California over the last 64 years.

This study focuses on analyzing trends in the annual peak discharge of thirty rivers divided into three regions of California: Northern coast, Southern coast, and Sierra Nevada Mountain region. The rivers selected have records that include years 1950-2014, and peak flows are minimally regulated, meaning dams or diversions upstream of the gaging point have little effect on the timing and volume of peak flows in the river. Ten rivers are analyzed in each region. Additionally, the period of record for each gage is split into two time periods, 1950-1981 and 1982-2014, both time periods are based on the water year. Years prior to 1950 were not included in the analysis because records for years prior to 1950 are less consistent in length, which would lead to many gaps in the data. These time periods were also chosen because the statistical analysis is simplified by having an equal number of years of recorded data. Statistical tests are used to evaluate differences between trends in annual peak flow among the locations and time periods. The analysis provides information regarding whether flood intensities are changing over time and, if so, whether the trends are significant.

STUDY AREA

The present study focuses on rivers located within three geographic regions of California, referred to here as the Northern, Southern and Sierra Nevada Regions (Figure 1). These regions were selected because they are influenced by different patterns of precipitation and runoff that produce floods of variable frequency and intensity. Sites are listed in Table 1 along with several drainage basin characteristics.

Figure 1. Location map of study in California.

Table 1. USGS sites selected for peak flow analysis.

River	USGS Site Number	Drainage Area (Km^2)	Gage Datum (m)
Northern			
Russian	11467000	3465	6
Mattole	11469000	635	15
Noyo	11468500	275	4
Van Duzen	11478500	575	109
Redwood	11482500	588	2
Smith	11532500	1590	24
Navarro	11468000	785	1
Eel	11477000	8063	11
Little	11481200	105	5
SF Eel	11476500	1391	66
Sierra Nevada			
Cole	11315000	54	17
Pitman	11237500	59	18
Bear	11230500	136	41
MF Stanislaus	11292700	743	227
Spanish	11402000	477	145
NF American	11427000	886	270
N Yuba	11413000	648	197
Sagehen	10343500	27	8
Merced	11264500	469	143
MF Mokelumne	11317000	177	54
Southern			
Sweetwater	11015000	118	36
Santa Maria	11028500	149	45
Sespe	11113000	653	199
Arroyo Seco 1	11152000	632	193
Big Sur	11143000	120	37
San Lorenzo	11160500	275	84
Pescadero	11162500	119	36
Arroyo Seco 2	11098000	41	13
Santa Cruz	11124500	192	58
Sisquoc	11138500	728	222

Precipitation patterns vary between the regions. The mean annual precipitation is usually higher on the coast but it receives lower intensity rainfall compared to inland regions such as the Sierra mountain range (Pitlick, 1994). The Northern region receives most precipitation between October and May, which is associated with Pacific frontal storms (Paulson et al., 1991). The average annual precipitation in the Northern region is 47 to 138cm (Perica et al., 2011). The average precipitation in the Southern region receives an average of 12-32cm annually (Perica et al., 2011). The Sierra Nevada Mountain range cause strong orographic effects and precipitation at higher elevation can be very intense, by either rain or snow (Pitlick, 1994). In winter conditions, the Sierra Nevada can accumulate snow to great depths with the relatively higher elevations reaching annual averages equaling 55-118cm and the lower, more southern, areas averaging 47-68cm (Perica et al., 2011). Flows occur during spring, because of snowmelt, but the greatest intensity flows occur during the winter months when rain-on-snow events occur. Rain on snow occurs when there is heavy rainfall coupled with partial melting of an existing snow pack (Pitlick, 1994).

The three regions chosen for this research have varying rock types and soil properties. The Northern region is underlain primarily by Mesozoic sedimentary and metasedimentary rocks, while the Southern is underlain by a mix of Mesozoic and Cenozoic sedimentary rocks and Quaternary alluvium (Jennings, 2010). The Sierra region consists of predominately granitic rock that is Mesozoic in age (Jennings, 2010).

The vegetation between the regions differs greatly. The Northern region can be classified overall as the Pacific Coniferous Forest, including predominately oak and redwood trees (Easter, 2004). The Southern region is dominated by urban areas, but there are zones of Chaparral and small areas of California grassland and agricultural areas (Easter, 2004). The Sierra region can be classified as a lower montane forest on the east slopes with oak woodland dominating on the east slopes (Easter, 2004).

METHODS

Ten site locations were chosen in each of the three regions discussed above. All site locations were chosen from the USGS database of annual peak flows. Sites were chosen to avoid large upstream diversions or dams. Data on annual peak flows were chosen for years 1950-2014. The data were then separated into two time periods: 1950-1981 and 1982-2014.

A series of statistical tests were used to evaluate the significance of differences in peak flows between the two time periods. T-tests were used to test the hypothesis that peak flows have increased over time, as expected if climate change is resulting in an increase in heavy precipitation and flooding. The normality of each data set was tested using the Shapiro-Wilk Test, a nonparametric test specifically used to test normality, which tested each river and each time period separately. Results from initial tests indicated that in most cases the untransformed values of peak discharge were not normally distributed, therefore, the logarithm of each value was used in applying the Shapiro-Wilk Test (Table 1). To aid in visualizing the results of the Shapiro-Wilk tests, Normal Quantile (Q-Q) plots of the logarithm of Q, were generated for each site. These graphs were used to assess normality by plotting the sample quantile on the vertical axis against the theoretical quantile on the horizontal axis. The sample quantile acts as the observed data point (the z-score) and the theoretical quantile is the expected z-score for the data point when it is assumed that the data comes from a normal distribution. If the sample quantiles match the theoretical quantiles the plot will depict a straight line, thereby indicating that the data follow a normal distribution. Normality is important because t-tests require that the data are normally distributed, independent of other observations, and continuous. A series of t-tests was then run on the normalized data to compare the mean annual peak flows between the two time periods at each site.

A second series of Q-Q plots was created to compare the sample quantiles of 1950-1981 (horizontal axis) against the sample quantiles of 1982-2014 (vertical axis). To do this, each data set was reviewed to determine whether the discharge records had the same number of years; if not, the lowest discharges were omitted until the record lengths were equal. The discharges for each time period were then ordered from lowest to highest, and the exceedance probability for each value was calculated: $p=m/(n+1)$, where m is the rank and n is the number of years of record. Thus the quantiles associated for each rank are equal. The Q-Q plots generated in this case compare differences in discharge which have the same quantile. When we graph the discharge values for the two time periods, 1950-1981 versus 1982-2014, we should see a 1-1 line if there are no differences in the discharge values. However, if peak flows are changing, there will be deviations from the 1-1 line.

RESULTS

Assessing Normality

Examples of Q-Q plots are shown for each region in Figure 2. In these plots, quantiles of the log-transformed values of peak discharge are plotted against quantiles of the standard normal distribution for two time periods, 1950-1981, and 1982-2014. The scatter around the straight lines gives an indication of whether the sample values come from a normal distribution. In the top two plots, the scatter around the straight lines is relatively large, suggesting that the log-transformed values of discharge are not normally distributed. It can be seen that Redwood Creek, 1950-1981, does not closely follow the line showing the data is not normal, whereas Redwood Creek 1982-2014 is similar but follows the line more closely and is normal. Both time periods for Cole Creek show a close correlation between the points and the lines, showing a normal distribution. There are deviations from the line at the higher magnitudes for Cole Creek 1950-1981, Bug Sur 1950-1981 and Big Sur 1982-2014, however these deviations are not great enough to skew the data from being a normal distribution.

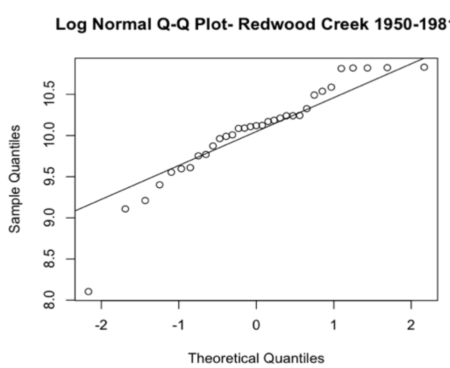

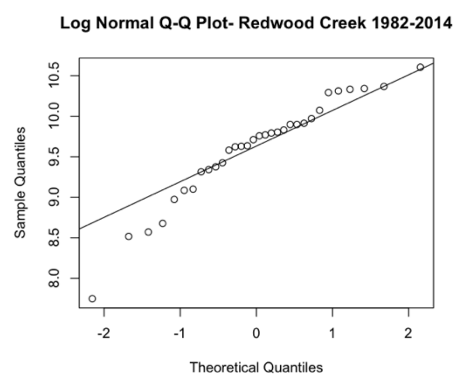

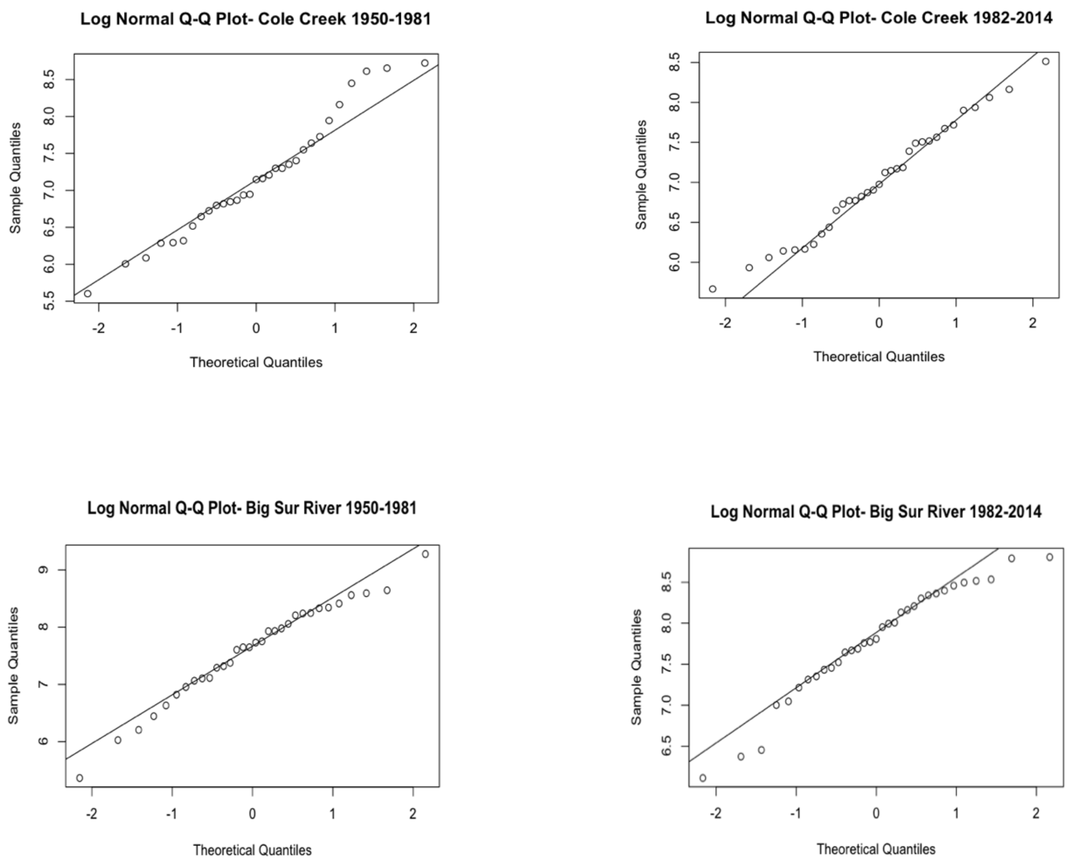

Figure 2. Q-Q plots for one river of each region. All plots show a normal distribution except Redwood Creek, 1950-1981.

The results of the Shapiro-Wilk test (Table 2) provide a more quantitative assessment of the normality of the data sets. None of the Northern region 1950-1981 data is normal, and there are a few other other sites between the other two regions which are not normal. However, the logarithm of the data proved to be normal in the majority of rivers (Table 2).

Table 2. Results of the Shapiro-Wilk test for normality. W is the Shapiro-Wilk test stastic significance probability. Values of p >0.05, highlighted in bold indicate data sets that are normally distributed.

	1950-1981		1982-2014	
River	W	p	W	p
Northern Region				
Russian	0.692	< 0.001	0.979	**0.755**
Mattole	0.863	< 0.002	0.963	**0.322**
Noyo	0.848	< 0.003	0.980	**0.798**
Van Duzen	0.799	< 0.004	0.962	**0.320**
Redwood	0.909	0.009	0.938	**0.066**
Smith	0.912	0.011	0.886	0.003
Navarro	0.862	< 0.001	0.965	**0.366**
Eel	0.813	< 0.001	0.958	**0.226**
Little	0.849	0.001	0.941	**0.081**
SF Eel	0.857	< 0.001	0.974	**0.617**
Sierra Nevada Region				
Cole	0.969	**0.482**	0.982	**0.835**
Pitman	0.967	**0.414**	0.972	**0.549**
Bear	0.956	**0.206**	0.956	**0.206**
MF Stanislaus	0.934	**0.095**	0.955	**0.186**
Spanish	0.912	0.012	0.969	**0.450**
NF American	0.949	**0.139**	0.973	**0.581**
N Yuba	0.979	**0.748**	0.978	**0.753**
Sagehen	0.979	**0.835**	0.979	**0.753**
Merced	0.960	**0.270**	0.969	**0.461**
MF Mokelumne	0.951	**0.150**	0.970	**0.476**
Southern Region				
Sweetwater	0.955	**0.327**	0.979	**0.742**
Santa Maria	0.939	**0.107**	0.936	**0.052**
Sespe	0.945	**0.106**	0.922	0.043
Arroyo Seco 1	0.716	< 0.001	0.964	**0.329**
Big Sur	0.974	**0.610**	0.949	**0.124**
San Lorenzo	0.930	0.039	0.954	**0.171**
Pescadero	0.926	0.037	0.355	0.050
Arroyo Seco 2	0.978	**0.749**	0.960	**0.266**
Santa Cruz	0.886	0.003	0.879	0.002
Sisquoc	0.882	0.002	0.935	**0.116**

Significance of Differences in Average Annual Peak Discharge

The results of the t-tests (Table 3) show that for a majority of sites (90%), the differences in average annual peak discharge between the two time periods are not statistically significant, $p > 0.05$. The Northern region has two rivers, the Redwood Creek and Smith River which show significant differences in annual mean flood values. There was one site, NF American which also showed a significant difference in annual mean flood values. However, in all three cases the differences were decreases in flood magnitudes. No significant differences in flood magnitudes were found in the Southern region.

Table 3. Mean annual flood values for two time periods.

	Mean Annual Flood (logQ)			
River	1950-1981	1982-2014	t	p
Northern				
Russian	10.65	10.57	0.48	0.06
Mattole	10.47	10.21	1.83	0.07
Noyo	8.77	8.57	0.90	0.37
Van Duzen	9.97	9.87	0.08	0.44
Redwood	10.05	9.64	2.83	**0.01**
Smith	11.41	11.15	2.19	**0.03**
Navarro	9.72	9.73	-0.05	0.96
Eel	12.07	11.82	1.46	0.15
Little	8.52	8.23	1.90	0.06
SF Eel	10.87	10.54	1.94	0.06
Sierra Nevada				
Cole	7.16	7.02	0.74	0.46
Pitman	6.29	6.27	0.06	0.95
Bear	6.67	6.72	-0.31	0.76
SF Stanislaus	7.77	7.51	0.07	0.47
Spanish	8.47	8.35	0.49	0.62
NF American	11.41	11.15	2.19	**0.03**
N Yuba	8.92	8.90	0.13	0.90
Sagehen	4.62	4.54	0.56	0.58
Merced	7.99	7.94	0.37	0.71
MF Mokelumne	6.68	6.51	0.56	0.58
Southern				
Sweetwater	4.60	4.89	-0.49	0.63
Santa Maria	4.05	4.77	-0.88	0.38
Sespe	8.67	8.88	-0.47	0.64
Arroyo Seco 1	8.64	8.90	-0.81	0.42
Big Sur	7.59	7.90	-1.04	0.30
San Lorenzo	0.84	8.63	-0.70	0.49
Pescadero	7.29	7.73	-1.51	0.14
Arroyo Seco 2	6.32	6.01	0.84	0.40
Santa Cruz	6.55	6.62	-0.15	0.88
Sisquoc	7.09	7.15	-0.14	0.89

Differences in Q-Q Plot Distributions

Additional patterns can be seen through the Q-Q plots which can depict changes in the extreme low flows and high flows, even if the mean is equal, as well as if the significant difference in the t-test was an increase or decrease.

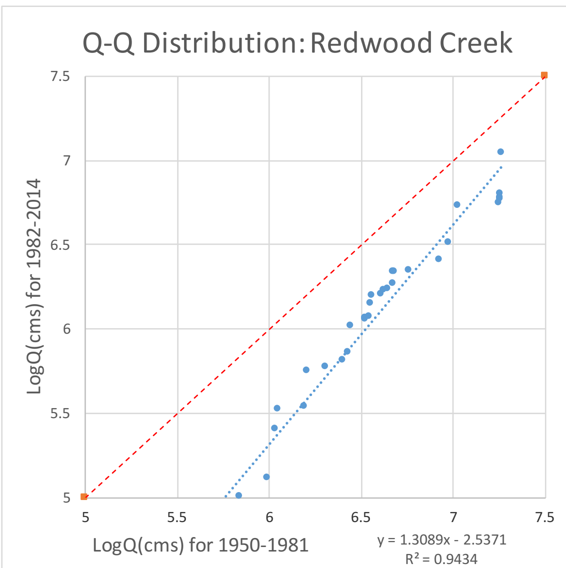

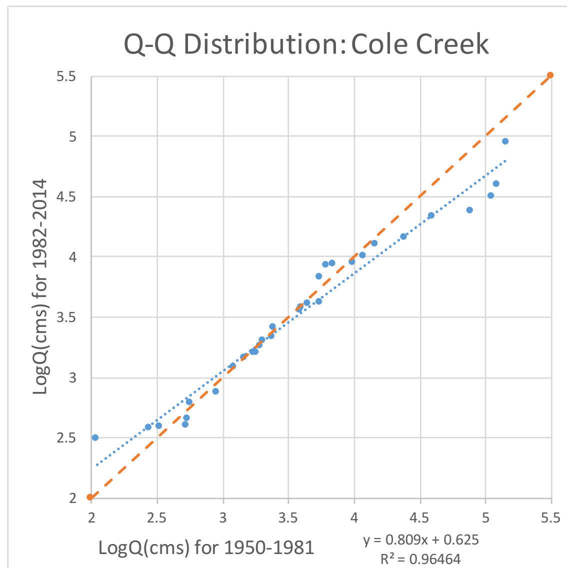

Figure 3. Q-Q plots comparing the distributions of flood magnitudes for two time periods, 1950-1981 and 1982-2014. The red dashed line is the 1-1 line and the blue dashed line is the trend line for the data.

Examples of Q-Q plots for Redwood Creek and Cole Creek are shown in Figure 3. For Redwood Creek, it is clear that the data do not follow the one-to-one line and thus depicts a significant difference in annual peak flow magnitudes. Additionally, because the points lie below the line, the plot indicates a decrease in flood magnitude over time. Figure 3, Cole Creek from the Sierra Nevada region, depicts the data points falling on or very near the one-to-one line depicting that there is no, or relatively little, change in flood magnitudes. However, even though the median magnitudes are approximately equal to the 1-1 line, there are deviations in the extreme low and high magnitudes. This demonstrates that there may be changing trends in the extreme values that t-tests cannot detect.

DISCUSSION

Ten percent of the site locations showed a significant decrease in annual peak floods. This could be due to a variety of factors including precipitation changes, artificial drainage ways, changes in vegetation, soil type, or other compounding factors. It can be seen from precipitation data from NOAA, that there seem to be no significant changes in precipitation patterns in any of the three regions (Figure 4). Other factors that could influence the results are that the rivers are various sizes and smaller rivers will be more influenced than larger rivers by changes in magnitude. More research needs to be conducted to understand why there seems to be a disconnect between the estimated increase in precipitation and the lack of evidence by floods. Additionally, the coast in the Southern region may not see increases due to the presence of sufficient man-made drainage whereas the Sierra region may not see increases due to raising temperatures which allow precipitation to fall in the form of rainfall in higher elevations, thus reducing snow pack and offsetting some of flow that would normally have flowed during the summer months.

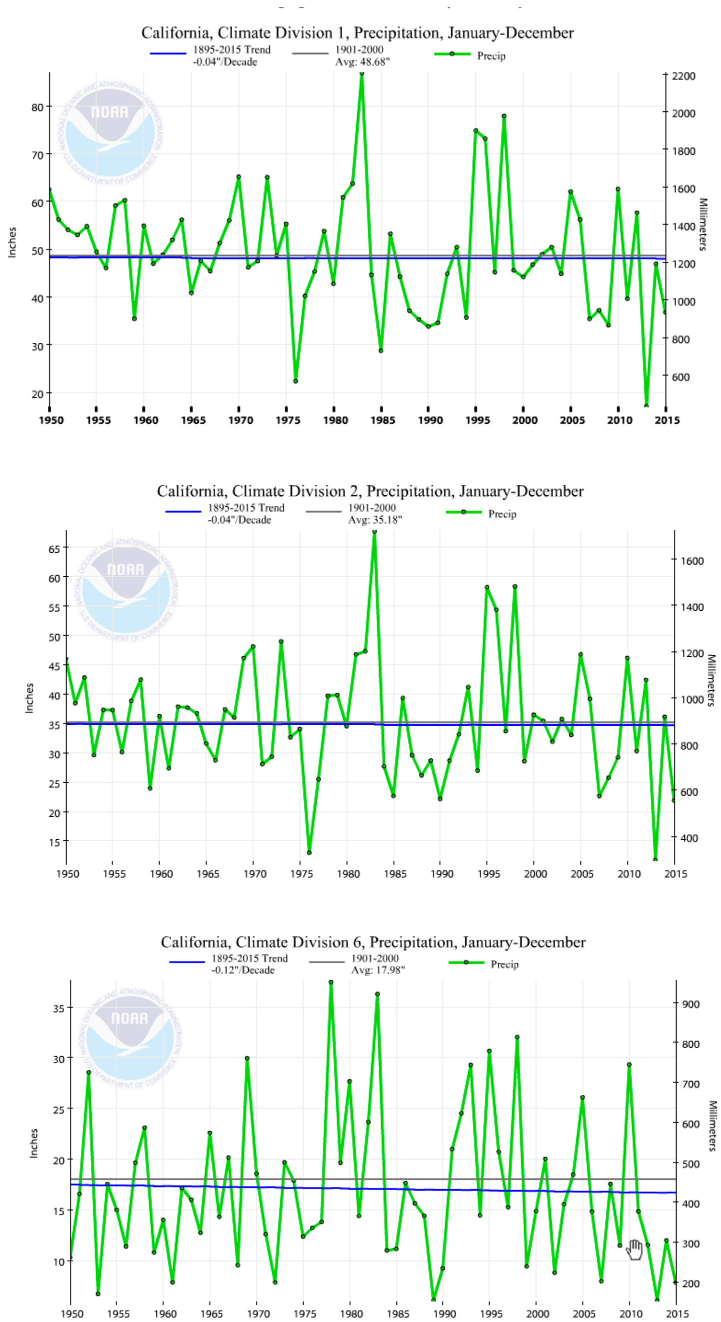

Figure 4. Precipitation data is shown for 1950-2014 for the Northern Coastal, Southern Coastal, and Sacramento drainage areas. The Sierra Nevada region does not have a specified drainage area, however the Sacrament drainage will capture most of the northern drainage area. The trend line for 1901-2000 is shown in blue and the trend line for 1895-2015 is shown in grey.

CONCLUSIONS

Changing flood magnitudes affect the safety of people, infrastructures, mitigation plans and surrounding ecosystems. 90% of the site locations did not experience a significant difference in annual flood magnitude. It can be concluded that few flood magnitudes are changing and in no particular spatial pattern. This is consistent with other flood studies, but is not consistent with an anticipated increase in precipitation intensity. Limitations to this study include the necessity to delete some of the lowest data points in order to have an equal number of data entries for each site, which may slightly vary the results. Understanding changes in flooding is important for the preparation in safety planning for citizens living in flood zones, and changes in ecosystems and surrounding habitats.

WORKS CITED

Dettinger, M.D., 20133: Climate change, atmospheric rivers, and floods in California- A multimodel analysis of storm frequency and magnitude changes. *J. Amer. Water Resour. Assoc.,* 47, 514-423.

Easter, Jeremiah. (2004). California vegetation/Wildlife Habitat Regions.

Hirsch, R.M. and Archfield, S.A., 2015, Flood trends: not higher but more often, *Nature Climate Change*, *5*(3), 198-199.

Kunkel, Kenneth E., David R. Easterling, Kelly Redmond, and Kenneth Hubbard, 2003, Temporal variation of extreme precipitation events in the United States: 1895-2000, Geography research letters 30, no. 17.

Jennings, C.W., with modifications by Gutierrez, C., Bryant, W., Saucedo, G., and Wills, C., (2010), *Geologic map of California*, California Geological Survey, Geologic Data Map No. 2, scale 1:750,000.

Kirkby, M.J., 1978. Implications for sediment transport. In: M.J. Kirkby (Editor), Hillslope Hydrology. Wiley-Interscience, New York, pp. 325 363.
PSHA California Geological Survey - Probablistic Seismic Hazards Assessment – Soils (PSHA California Geological Survey - Probablistic Seismic Hazards Assessment - Soils) http://www.conservation.ca.gov/cgs/rghm/psha/pages/soils.aspx

Mallakpour, I. and Villarini, G., 2015, The changing nature of flooding across the central United States, *Nature Climate Change*, *5*(3), 250-254.

NOAA National Centers for Environmental Information. 2015. Climate at a Glance- Time Series Data. March 22, 2016. http://www.ncdc.noaa.gov/cag/time-series/us/4/6/pcp/ytd/12/19502014?base_prd=true&firstbaseyear=1901&lastbaseyear=2000&trend=true&trend_base=10&firsttrendyear=1895&lasttrendyear=2016

NOAA National Weather Service. 2014, May14. Hydrologic Information Center- Flood Loss Data. Feb. 15, 2016. http://www.nws.noaa.gov/hic/

Perica, S., Dietz, S., Heim, S., Hiner, L., Maitaria, K., Martin, D., Pavlovic, S., Roy, I., Trypaluk, C., Unruh, D. and Yan, F. (2011), NOAA Atlas 14 Volume 6 Version 2.0, *Precipitation-Frequency Atlas of the United States, California*. NOAA, National Weather Service, Silver Spring, MD.

Peterson, T.C., Heim Jr, R.R., Hirsch, R., Kaiser, D.P., Brooks, H., Diffenbaugh, N.S., Dole, R.M., Giovannettone, J.P., Guirguis, K., Karl, T.R. and Katz, R.W., 2013. Monitoring and understanding changes in heat waves, cold waves, floods, and droughts in the United States: state of knowledge. *Bulletin of the American Meteorological Society*, *94*(6), 821-834.

Pitlick, John. "Relation between peak flows, precipitation, and physiography for five mountainous regions in the western USA." Journal of Hydrology 158.3 (1994): 219-240.

APPENDIX

FIGURES

Figure 4

4A

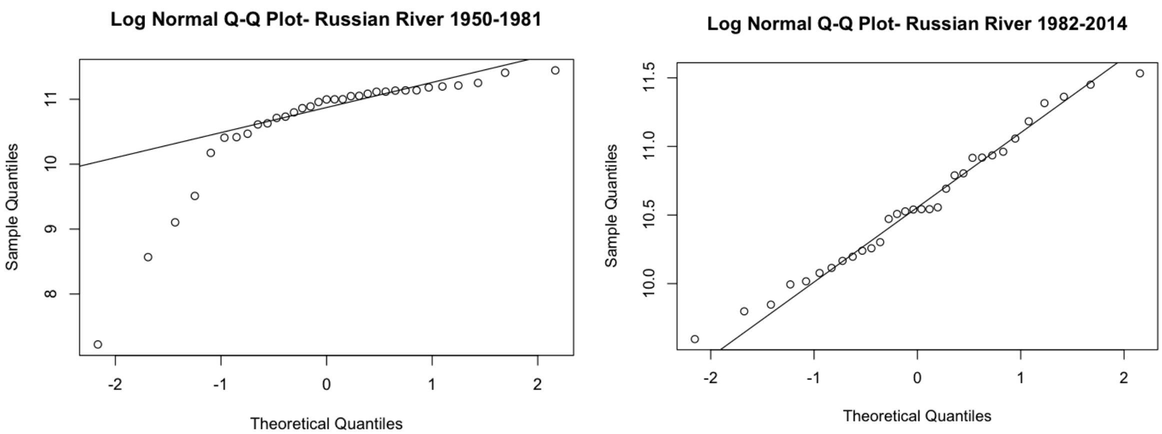

4B

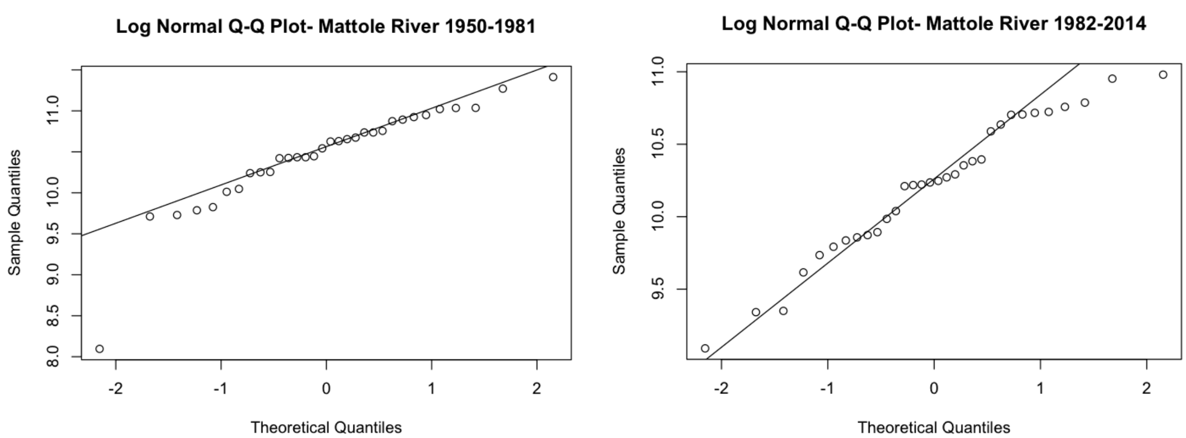

4C

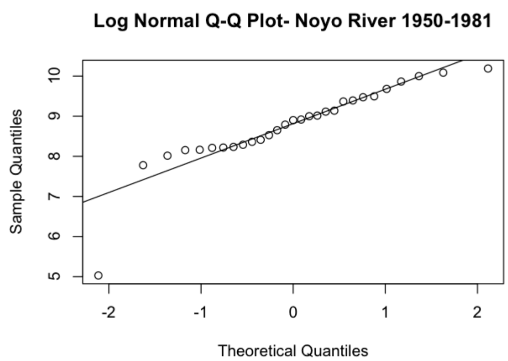
Log Normal Q-Q Plot- Noyo River 1950-1981
Sample Quantiles
Theoretical Quantiles
5
6
7
8
9
10
-2
-1
0
1
2

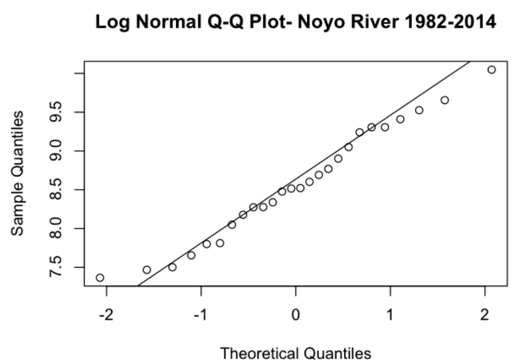
Log Normal Q-Q Plot- Noyo River 1982-2014
Sample Quantiles
Theoretical Quantiles
7.5
8.0
8.5
9.0
9.5
-2
-1
0
1
2

4D

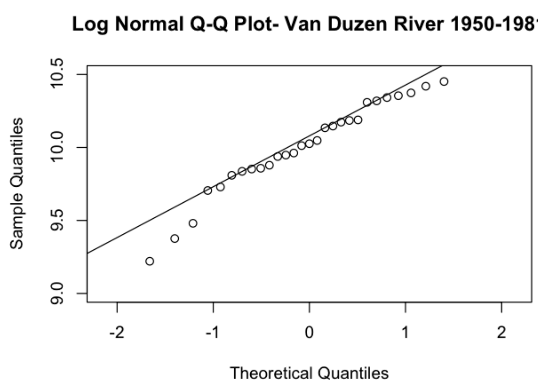
Log Normal Q-Q Plot- Van Duzen River 1950-1981
Sample Quantiles
Theoretical Quantiles
9.0
9.5
10.0
10.5
-2
-1
0
1
2

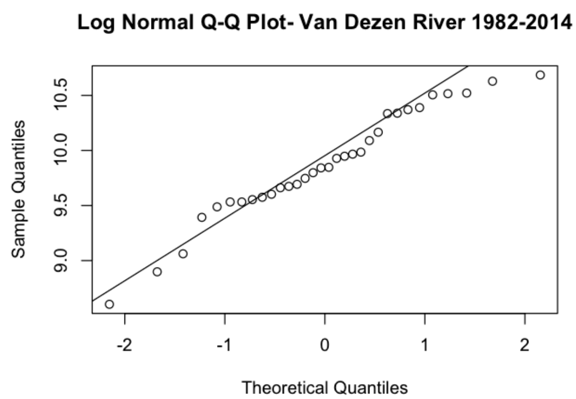
Log Normal Q-Q Plot- Van Dezen River 1982-2014
Sample Quantiles
Theoretical Quantiles
9.0
9.5
10.0
10.5
-2
-1
0
1
2

4E

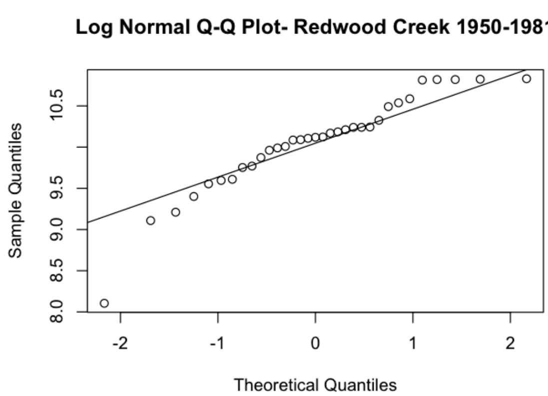
Log Normal Q-Q Plot- Redwood Creek 1950-1981
Sample Quantiles
Theoretical Quantiles
8.0
8.5
9.0
9.5
10.5
-2
-1
0
1
2

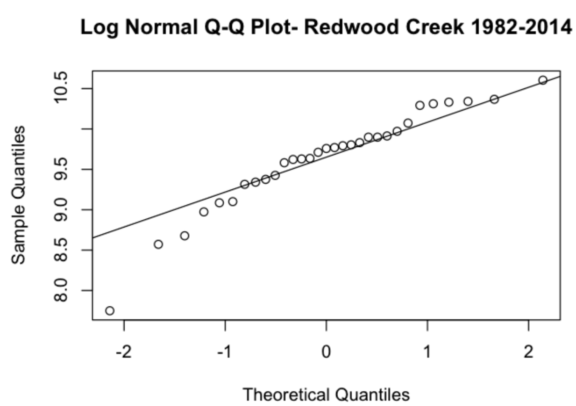
Log Normal Q-Q Plot- Redwood Creek 1982-2014
Sample Quantiles
Theoretical Quantiles
8.0
8.5
9.0
9.5
10.5
-2
-1
0
1
2

4F

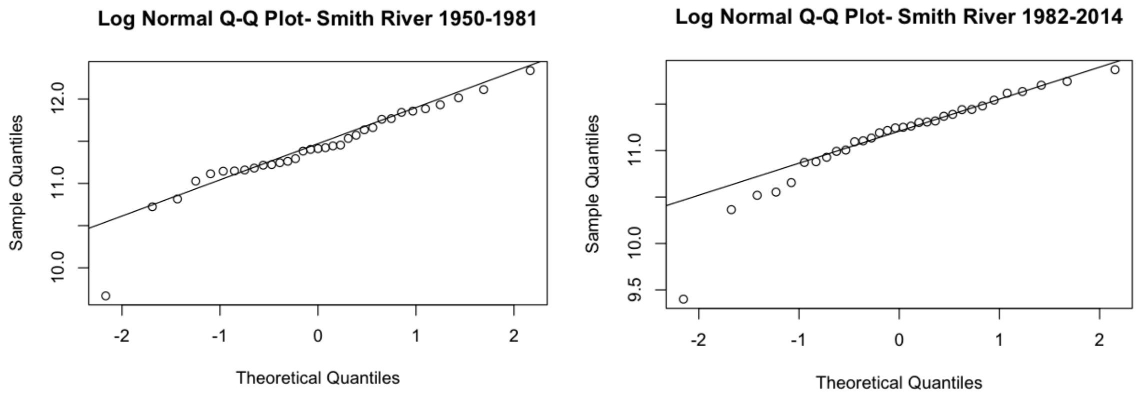
Log Normal Q-Q Plot- Smith River 1950-1981
Sample Quantiles
Theoretical Quantiles
Log Normal Q-Q Plot- Smith River 1982-2014
Sample Quantiles
Theoretical Quantiles

4G

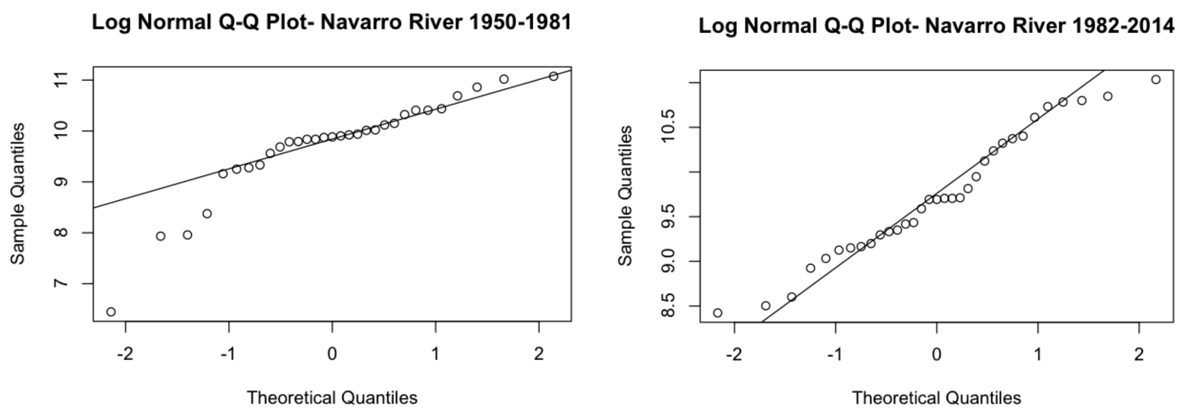
Log Normal Q-Q Plot- Navarro River 1950-1981
Sample Quantiles
Theoretical Quantiles
Log Normal Q-Q Plot- Navarro River 1982-2014
Sample Quantiles
Theoretical Quantiles

4H

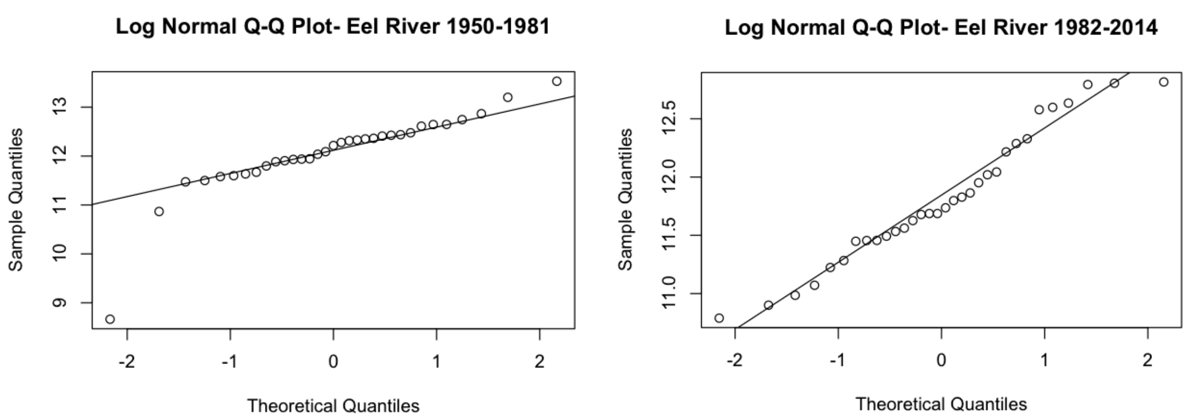
Log Normal Q-Q Plot- Eel River 1950-1981
Sample Quantiles
Theoretical Quantiles
Log Normal Q-Q Plot- Eel River 1982-2014
Sample Quantiles
Theoretical Quantiles

4I

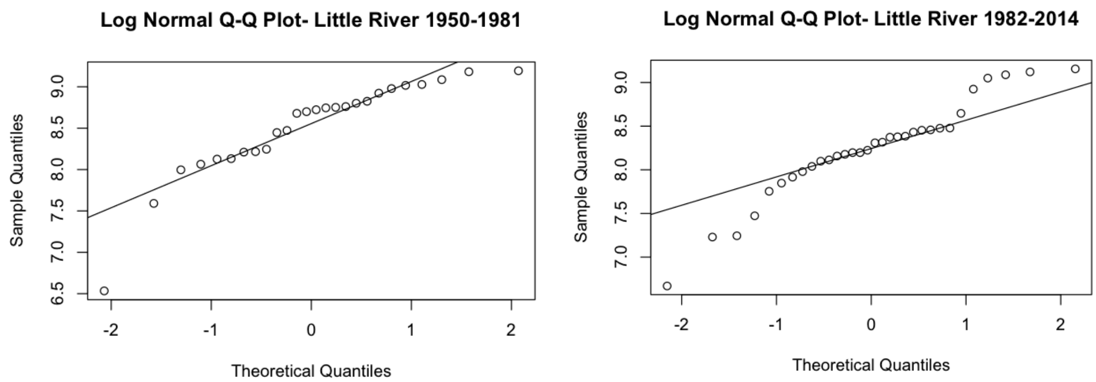

2J

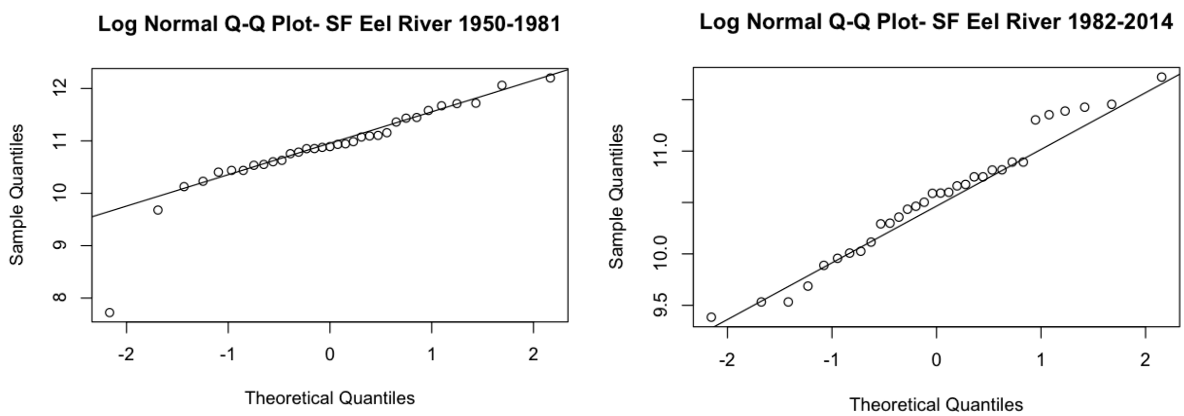

Figure 2 depicts the Normal Quantile plots for the Northern region. The logarithmic value of the data is on the y-axis while the theoretical, or the expected z-score for the data point x_i assuming the data is normal, is plotted on the x-axis. The trend line is displayed on the graph. If the data closely align with the trend line, the data distribution is normal, however if the data points do not the data is depicted as not normal.

Figure 5

5A

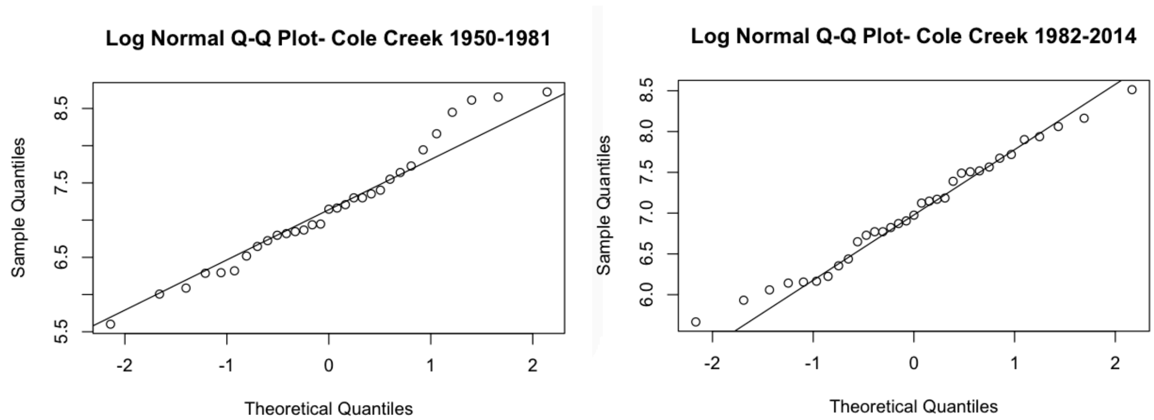

5B

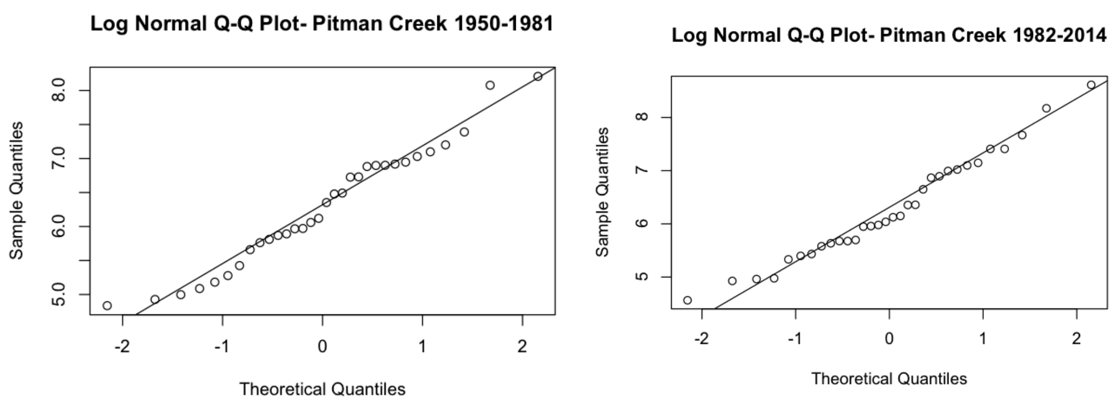

3C

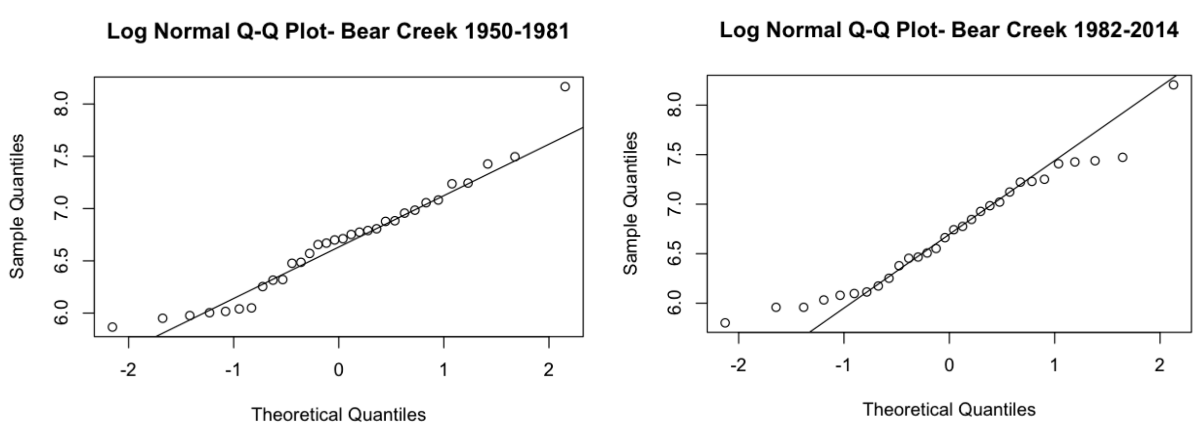

5D

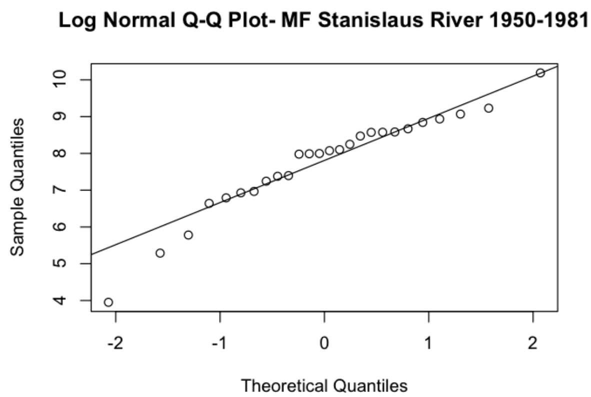
Log Normal Q-Q Plot- MF Stanislaus River 1950-1981
Sample Quantiles
Theoretical Quantiles
4
5
6
7
8
9
10
-2
-1
0
1
2

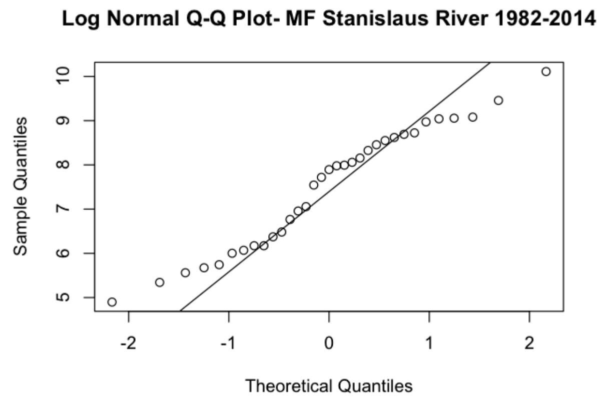
Log Normal Q-Q Plot- MF Stanislaus River 1982-2014
Sample Quantiles
Theoretical Quantiles
5
6
7
8
9
10
-2
-1
0
1
2

5E

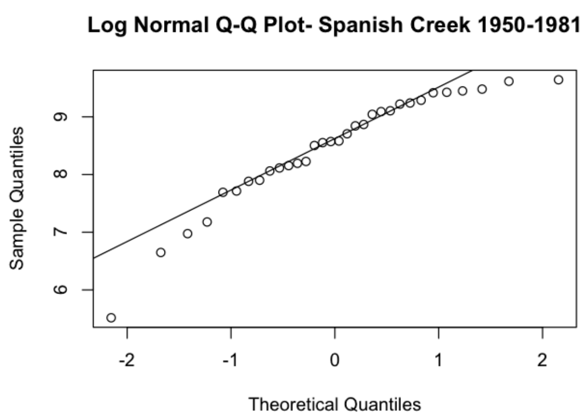
Log Normal Q-Q Plot- Spanish Creek 1950-1981
Sample Quantiles
Theoretical Quantiles
6
7
8
9
-2
-1
0
1
2

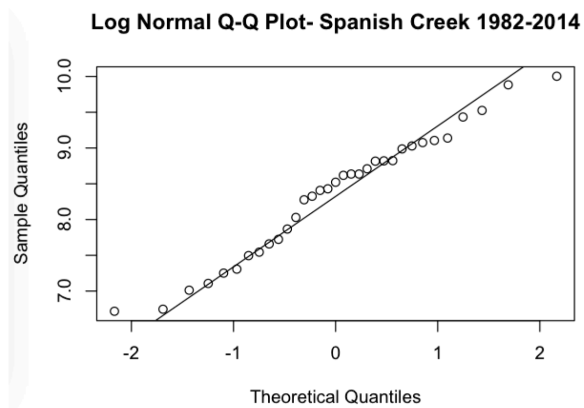
Log Normal Q-Q Plot- Spanish Creek 1982-2014
Sample Quantiles
Theoretical Quantiles
7.0
8.0
9.0
10.0
-2
-1
0
1
2

3F

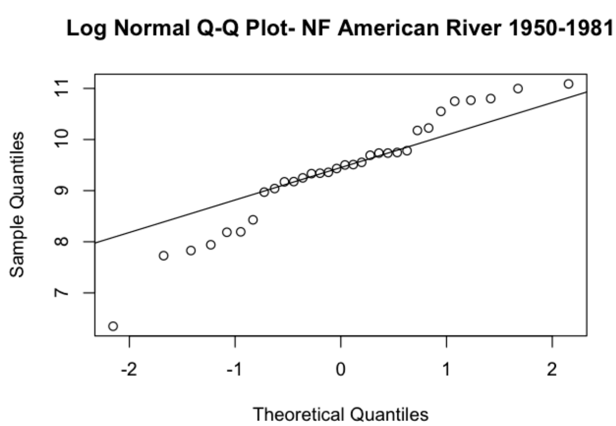
Log Normal Q-Q Plot- NF American River 1950-1981
Sample Quantiles
Theoretical Quantiles
7
8
9
10
11
-2
-1
0
1
2

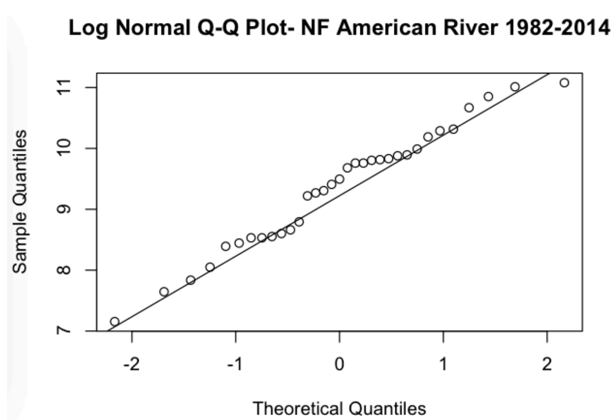
Log Normal Q-Q Plot- NF American River 1982-2014
Sample Quantiles
Theoretical Quantiles
7
8
9
10
11
-2
-1
0
1
2

5G

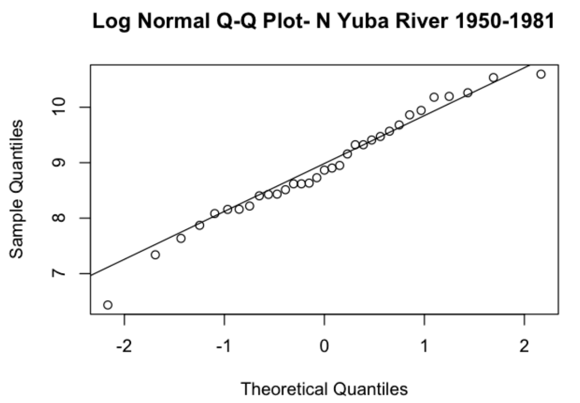
Log Normal Q-Q Plot- N Yuba River 1950-1981
Sample Quantiles
Theoretical Quantiles
-2 -1 0 1 2
7 8 9 10

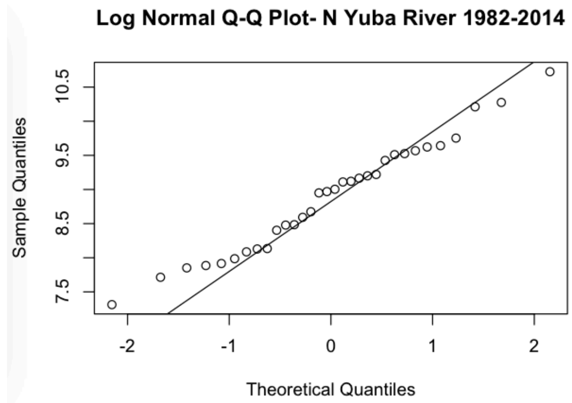
Log Normal Q-Q Plot- N Yuba River 1982-2014
Sample Quantiles
Theoretical Quantiles
-2 -1 0 1 2
7.5 8.5 9.5 10.5

5H

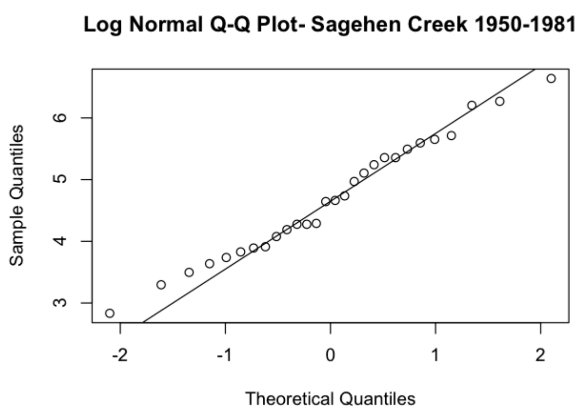
Log Normal Q-Q Plot- Sagehen Creek 1950-1981
Sample Quantiles
Theoretical Quantiles
-2 -1 0 1 2
3 4 5 6

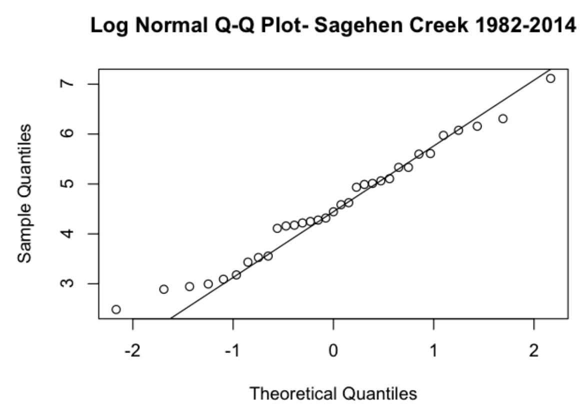
Log Normal Q-Q Plot- Sagehen Creek 1982-2014
Sample Quantiles
Theoretical Quantiles
-2 -1 0 1 2
3 4 5 6 7

5I

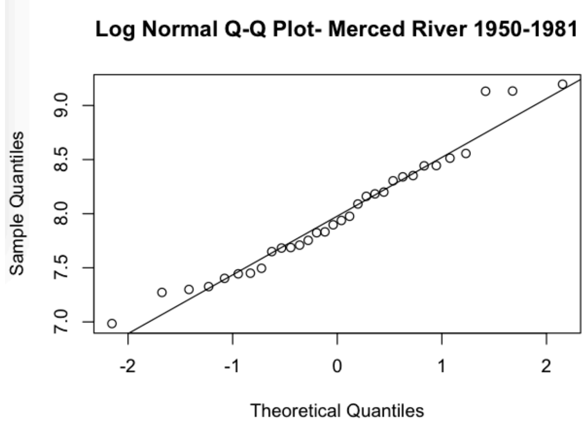
Log Normal Q-Q Plot- Merced River 1950-1981
Sample Quantiles
Theoretical Quantiles
-2 -1 0 1 2
7.0 7.5 8.0 8.5 9.0

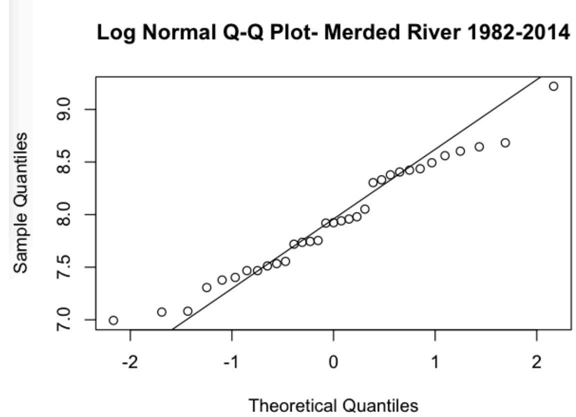
Log Normal Q-Q Plot- Merded River 1982-2014
Sample Quantiles
Theoretical Quantiles
-2 -1 0 1 2
7.0 7.5 8.0 8.5 9.0

5J

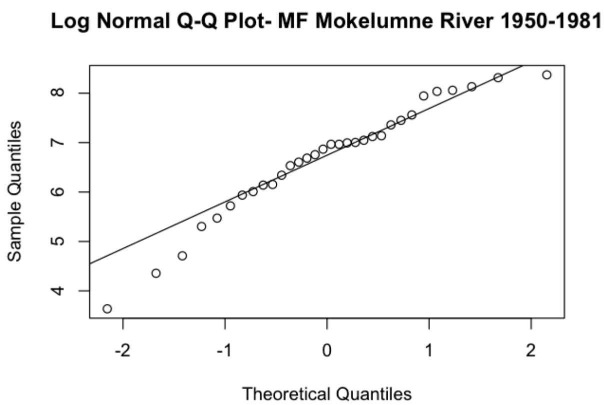

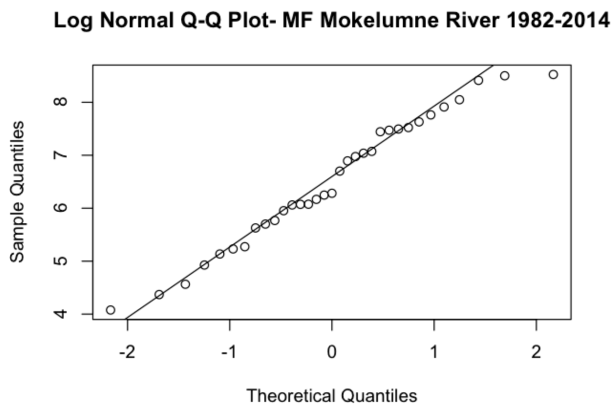

Figure 5 depicts the Normal Quantile plots for the Sierra Nevada region. The logarithmic value of the data is on the y-axis while the theoretical, or the expected z-score for the data point x_i assuming the data is normal, is plotted on the x-axis. The trend line is displayed on the graph. If the data closely align with the trend line, the data distribution is normal, however if the data points do not the data is depicted as not normal.

Figure 6

6A

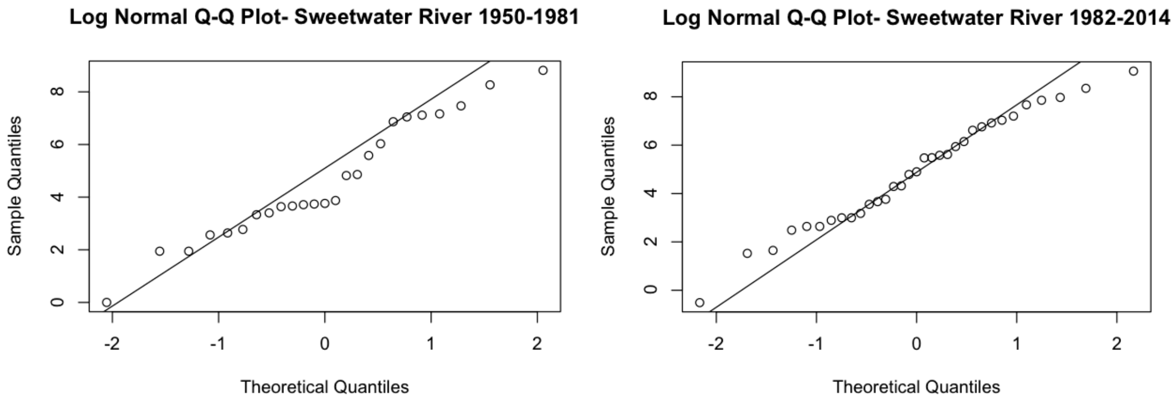

6B

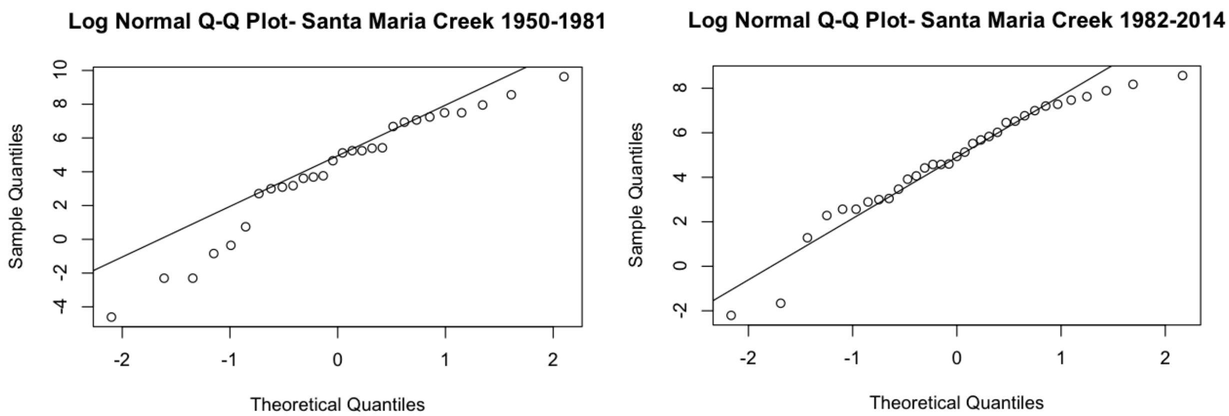

6C

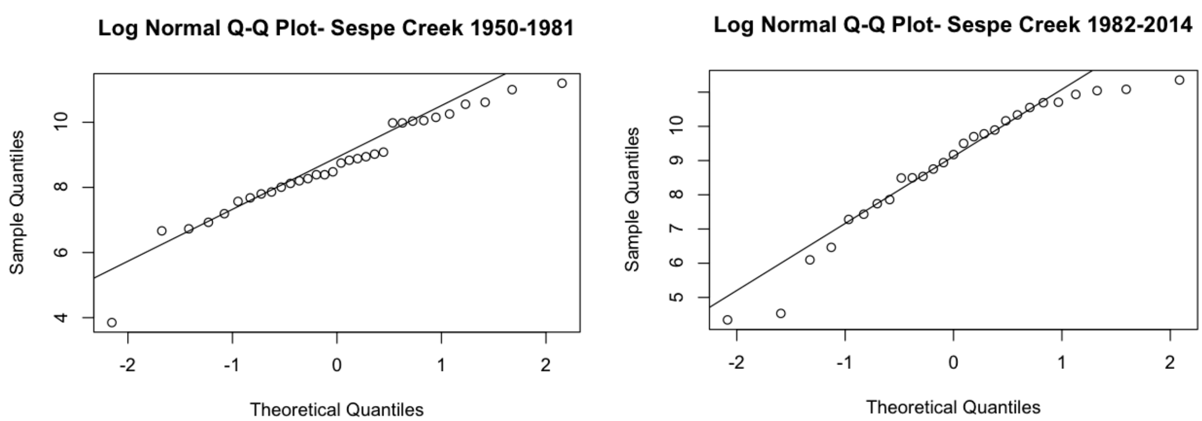

6D

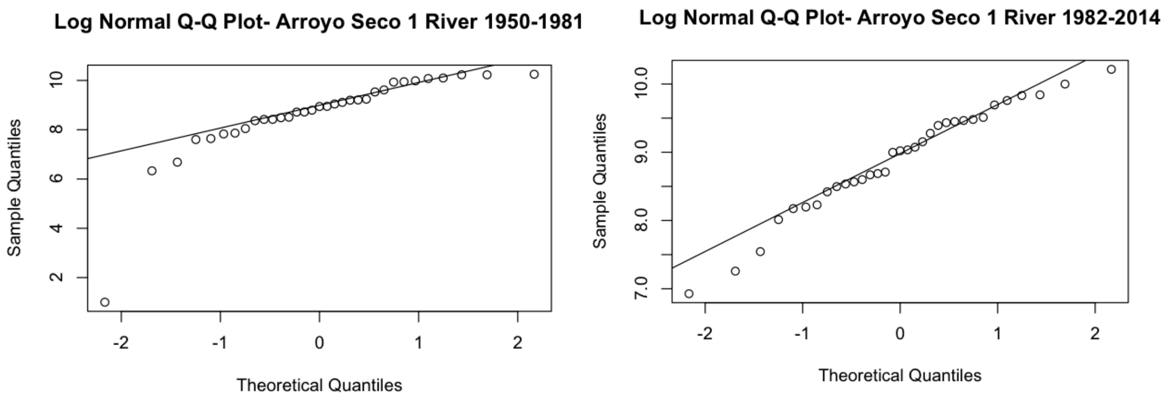

Log Normal Q-Q Plot- Arroyo Seco 1 River 1950-1981
Sample Quantiles
Theoretical Quantiles
Log Normal Q-Q Plot- Arroyo Seco 1 River 1982-2014
Sample Quantiles
Theoretical Quantiles

6E

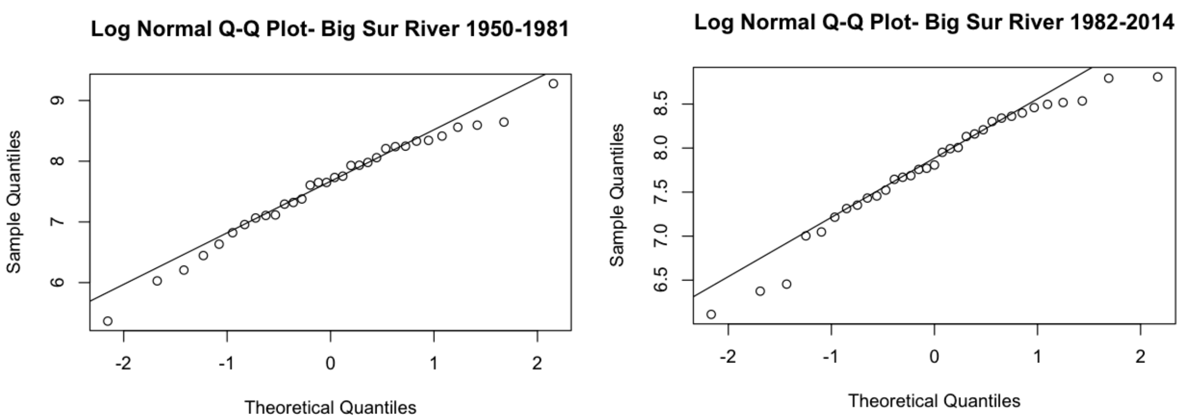

Log Normal Q-Q Plot- Big Sur River 1950-1981
Sample Quantiles
Theoretical Quantiles
Log Normal Q-Q Plot- Big Sur River 1982-2014
Sample Quantiles
Theoretical Quantiles

6F

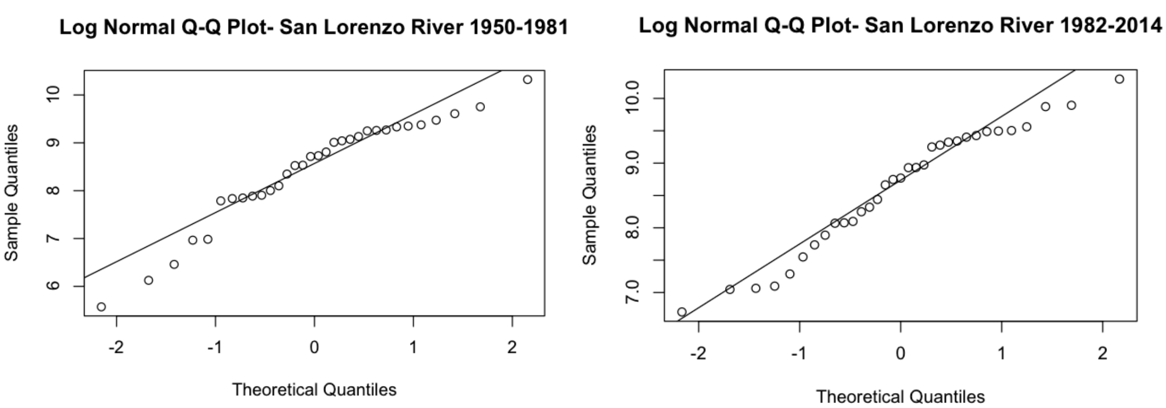

Log Normal Q-Q Plot- San Lorenzo River 1950-1981
Sample Quantiles
Theoretical Quantiles
Log Normal Q-Q Plot- San Lorenzo River 1982-2014
Sample Quantiles
Theoretical Quantiles

6G

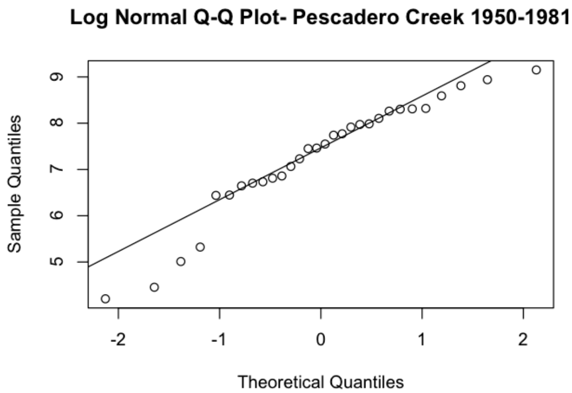
Log Normal Q-Q Plot- Pescadero Creek 1950-1981
Sample Quantiles
Theoretical Quantiles

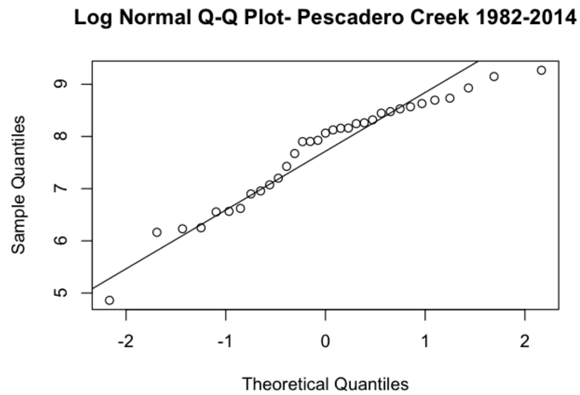
Log Normal Q-Q Plot- Pescadero Creek 1982-2014
Sample Quantiles
Theoretical Quantiles

6H

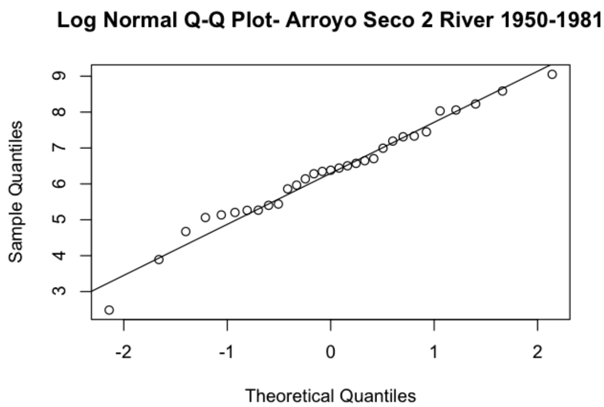
Log Normal Q-Q Plot- Arroyo Seco 2 River 1950-1981
Sample Quantiles
Theoretical Quantiles

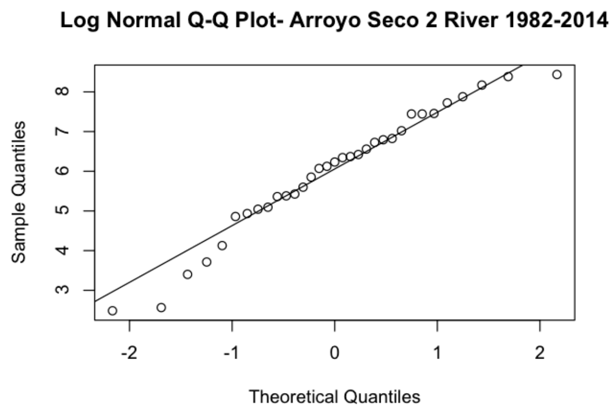
Log Normal Q-Q Plot- Arroyo Seco 2 River 1982-2014
Sample Quantiles
Theoretical Quantiles

6I

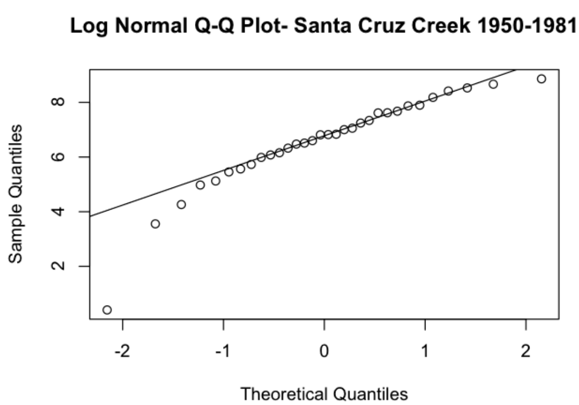
Log Normal Q-Q Plot- Santa Cruz Creek 1950-1981
Sample Quantiles
Theoretical Quantiles

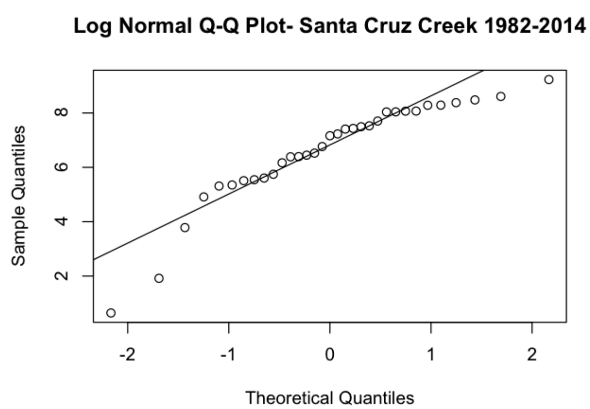
Log Normal Q-Q Plot- Santa Cruz Creek 1982-2014
Sample Quantiles
Theoretical Quantiles

6J

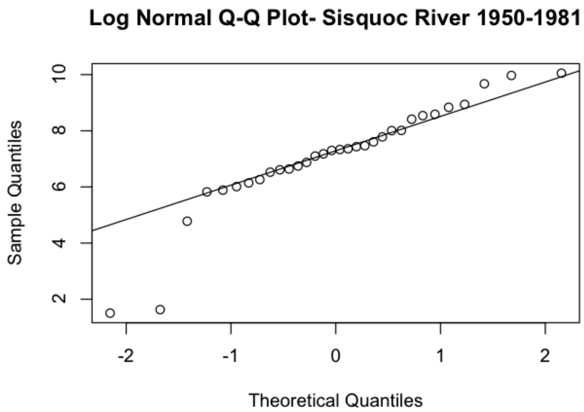

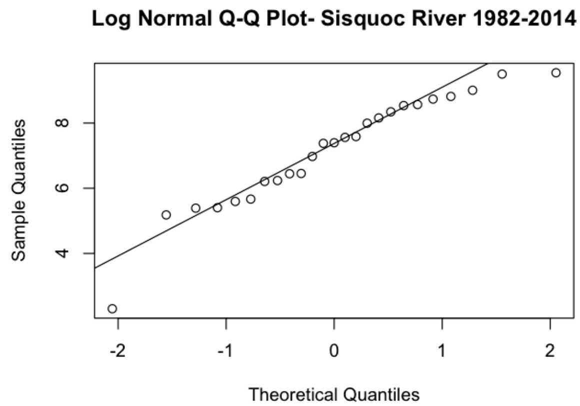

Figure 6 depicts the Normal Quantile plots for the Southern region. The logarithmic value of the data is on the y-axis while the theoretical, or the expected z-score for the data point x_i assuming the data is normal, is plotted on the x-axis. The trend line is displayed on the graph. If the data closely align with the trend line, the data distribution is normal, however if the data points do not the data is depicted as not normal.

Figure 7

7A

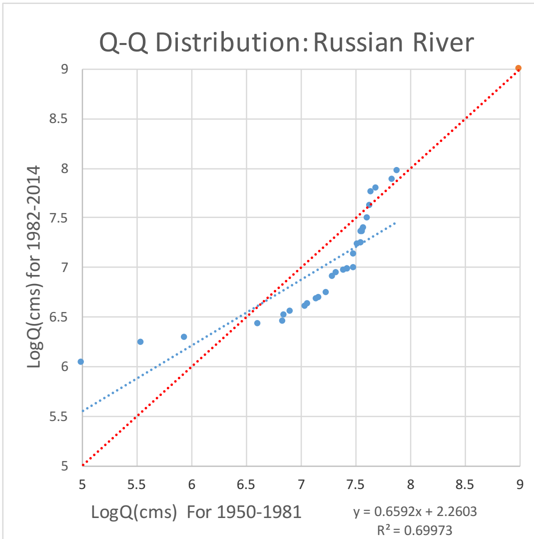

7B

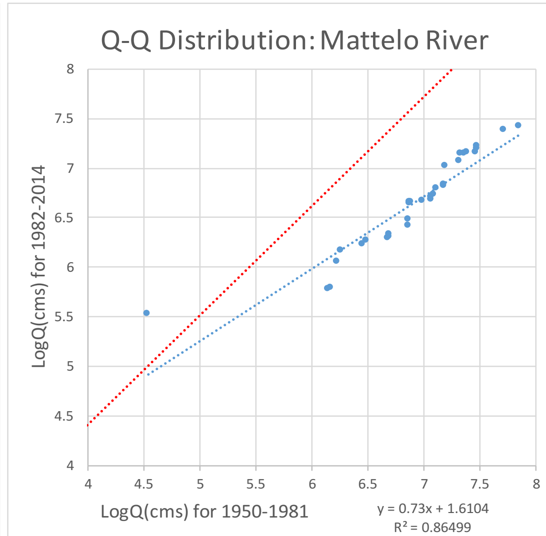

7C

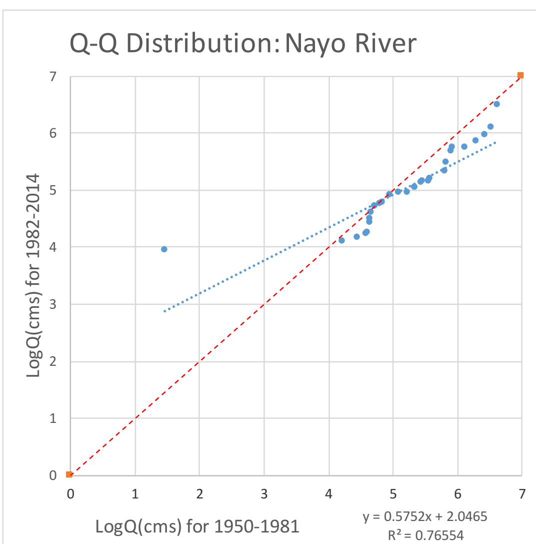

7D

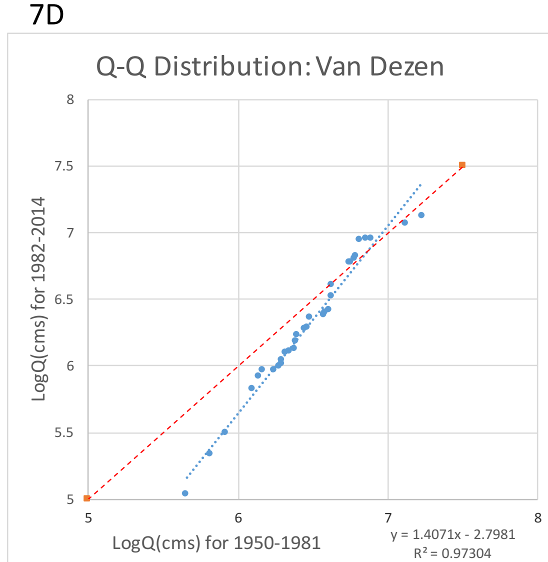

7E

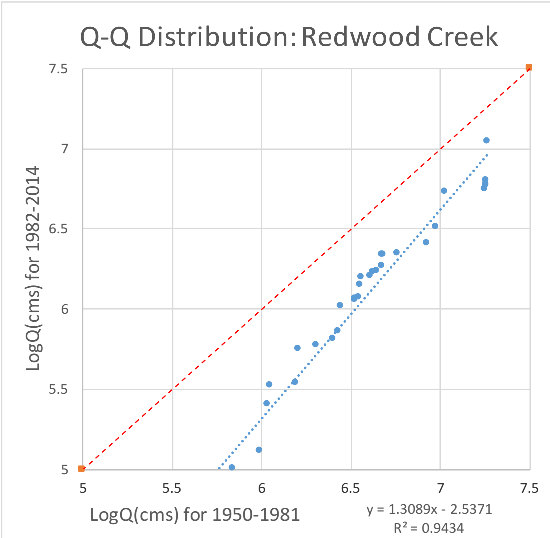
Q-Q Distribution: Redwood Creek
LogQ(cms) for 1982-2014
LogQ(cms) for 1950-1981
y = 1.3089x - 2.5371
R² = 0.9434

7F

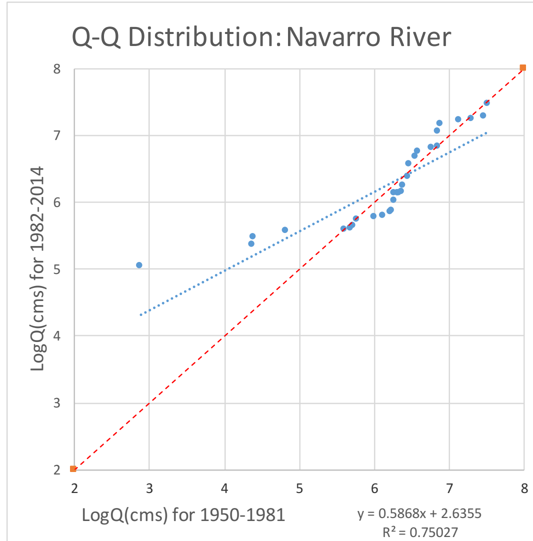
Q-Q Distribution: Navarro River
LogQ(cms) for 1982-2014
LogQ(cms) for 1950-1981
y = 0.5868x + 2.6355
R² = 0.75027

7G

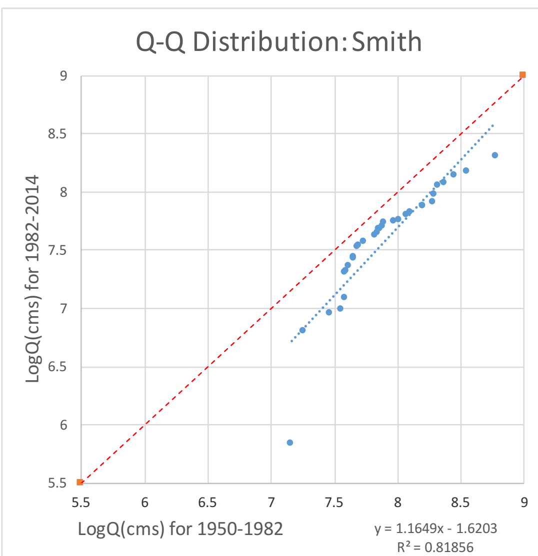
Q-Q Distribution: Smith
LogQ(cms) for 1982-2014
LogQ(cms) for 1950-1982
y = 1.1649x - 1.6203
R² = 0.81856

7H

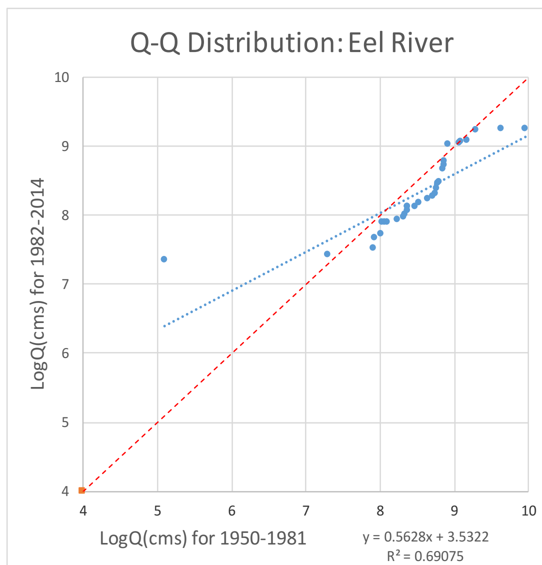
Q-Q Distribution: Eel River
LogQ(cms) for 1982-2014
LogQ(cms) for 1950-1981
y = 0.5628x + 3.5322
R² = 0.69075

7I

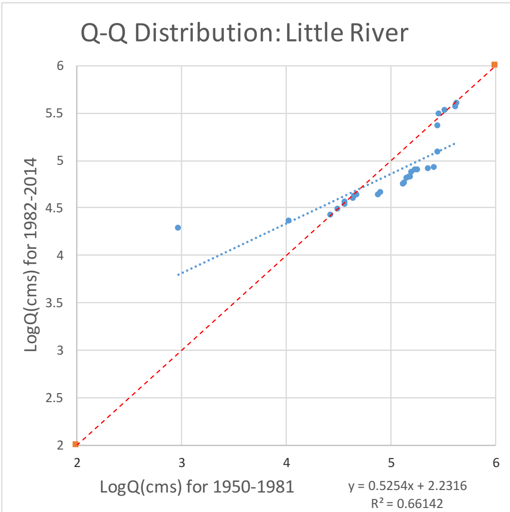

7J

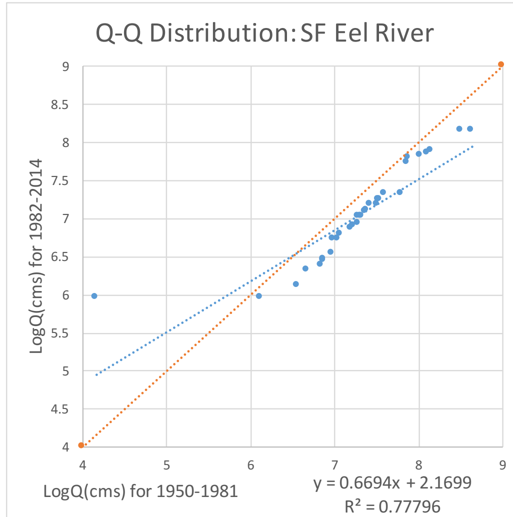

Figure 7A-J shows the Q-Q plot for the logarithmic values of the data for the Northern region. The 1-1 line is depicted as a dashed red line and the trend line for the data represented as a blue dashed line. The linear regression of the trend line and the R^2 are shown in the lower right corner of the graph.

Figure 8

8A

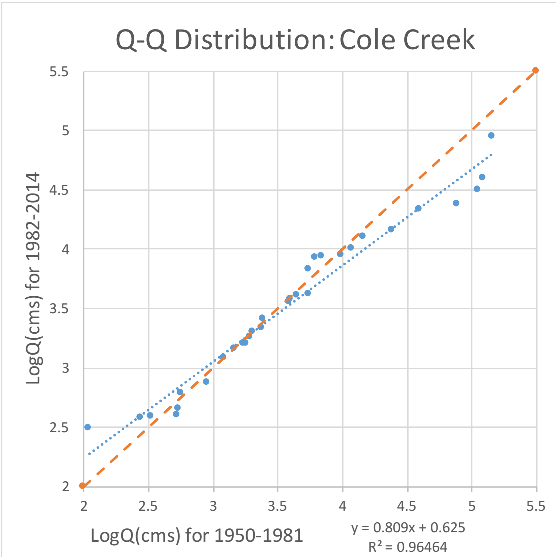

8B

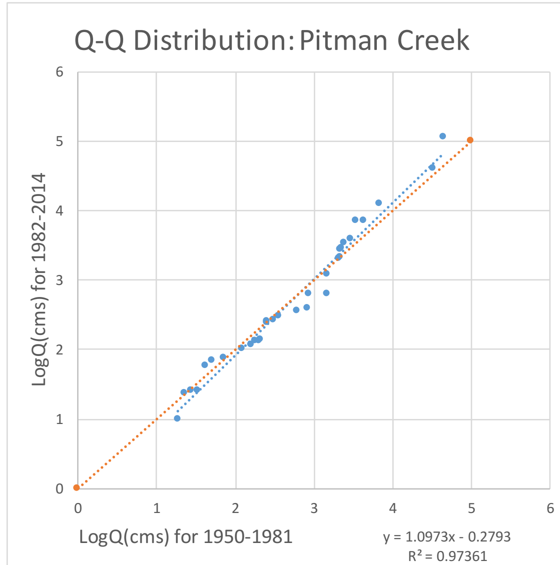

8C

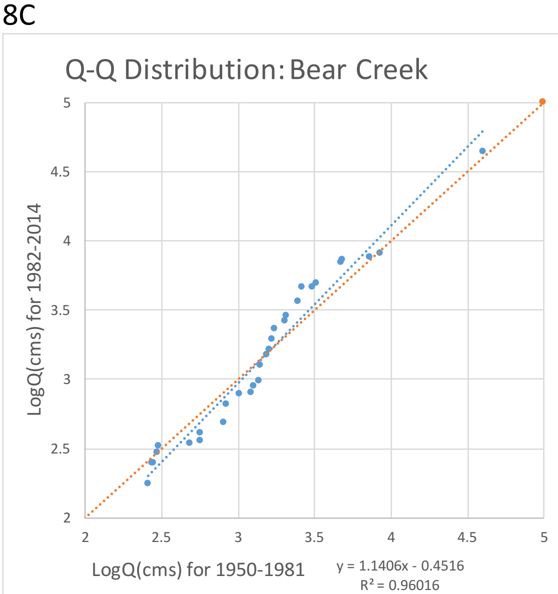

8D

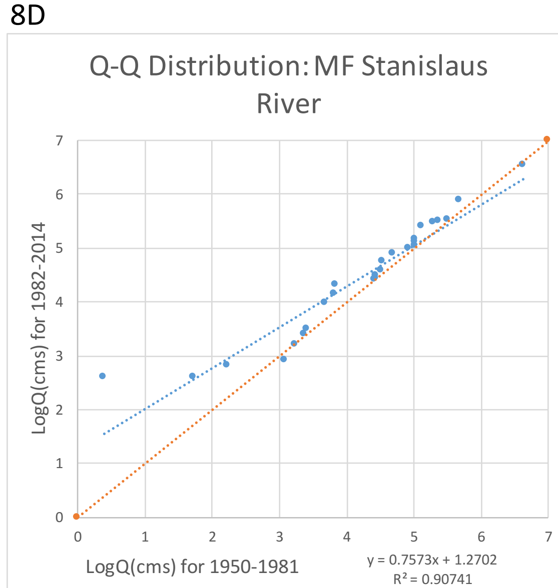

8E

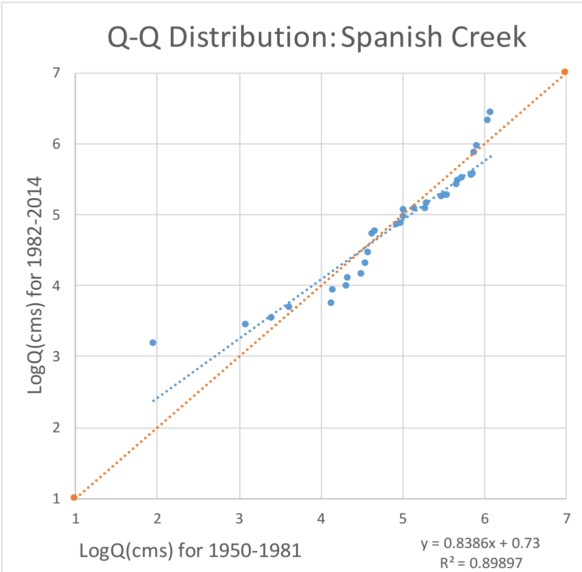
Q-Q Distribution: Spanish Creek
LogQ(cms) for 1982-2014
LogQ(cms) for 1950-1981
y = 0.8386x + 0.73
R² = 0.89897

8F

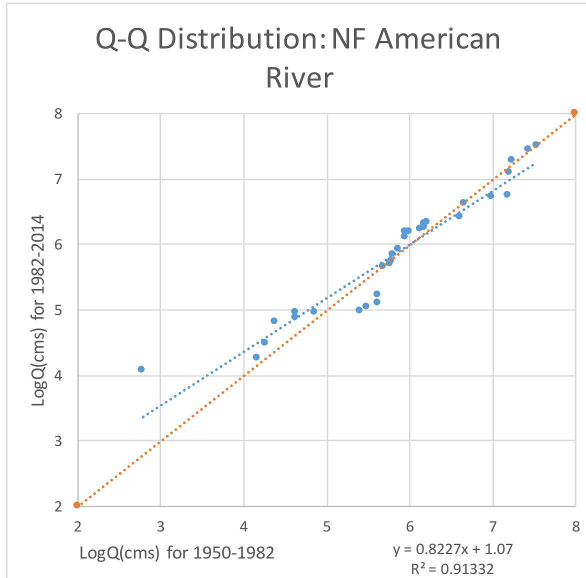
Q-Q Distribution: NF American River
LogQ(cms) for 1982-2014
LogQ(cms) for 1950-1982
y = 0.8227x + 1.07
R² = 0.91332

8G

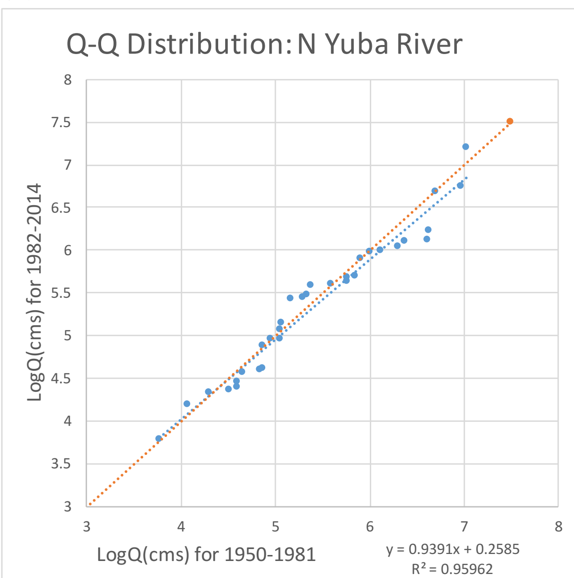
Q-Q Distribution: N Yuba River
LogQ(cms) for 1982-2014
LogQ(cms) for 1950-1981
y = 0.9391x + 0.2585
R² = 0.95962

8H

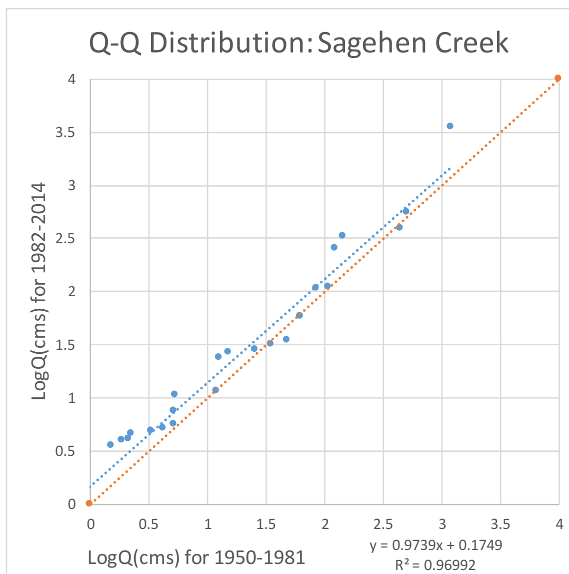
Q-Q Distribution: Sagehen Creek
LogQ(cms) for 1982-2014
LogQ(cms) for 1950-1981
y = 0.9739x + 0.1749
R² = 0.96992

8I

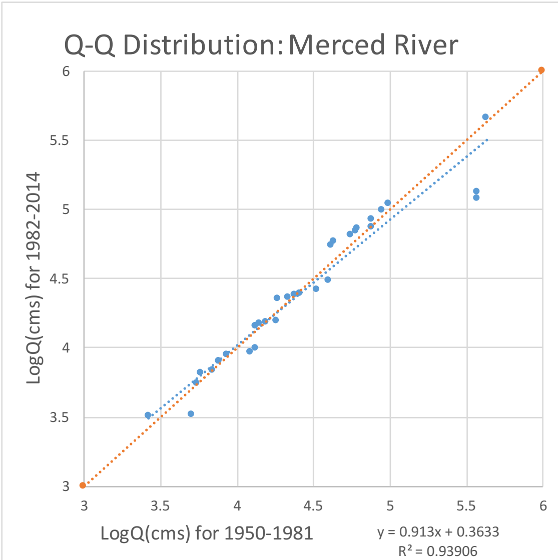

8J

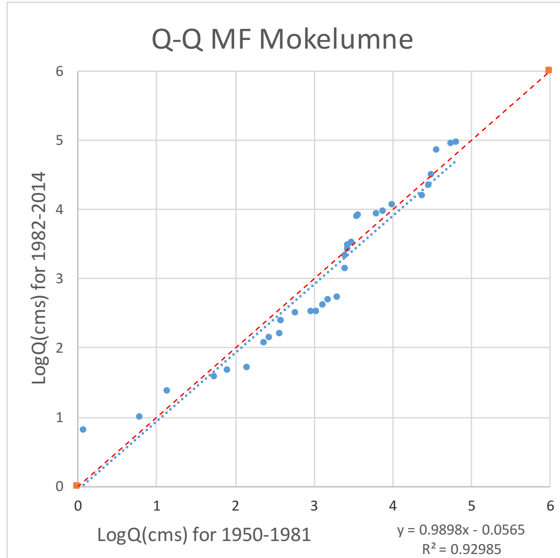

Figure 8A-J shows the Q-Q plot for the logarithmic values of the data for the Sierra Nevada region. The 1-1 line is depicted as a dashed red line and the trend line for the data represented as a blue dashed line. The linear regression of the trend line and the R^2 are shown in the lower right corner of the graph.

Figure 9

9A

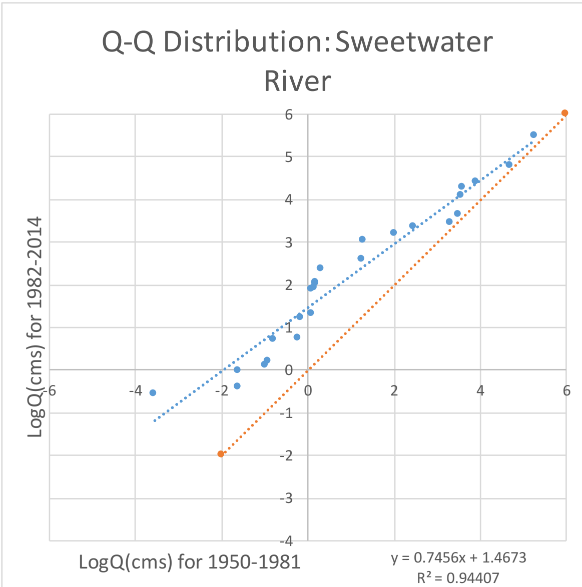

9B

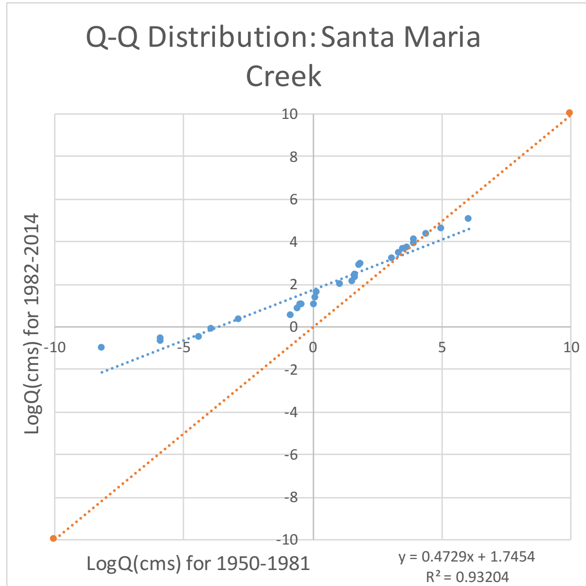

9C

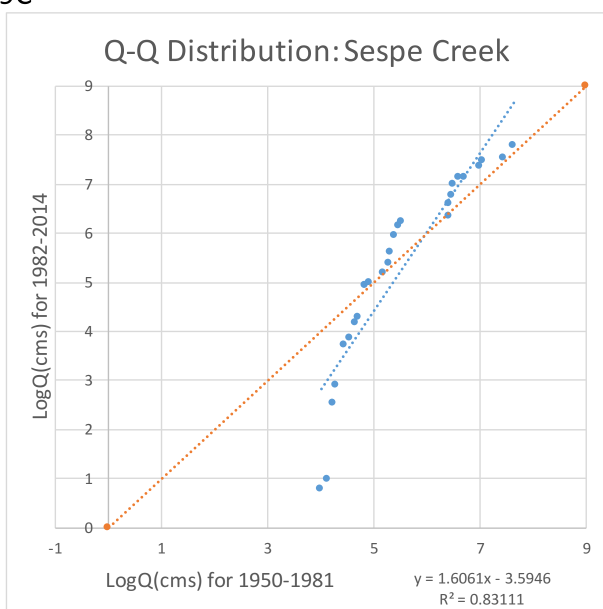

9D

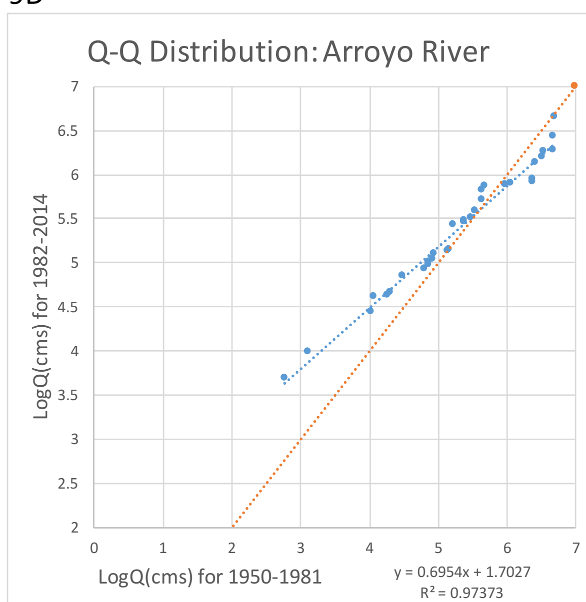

9E

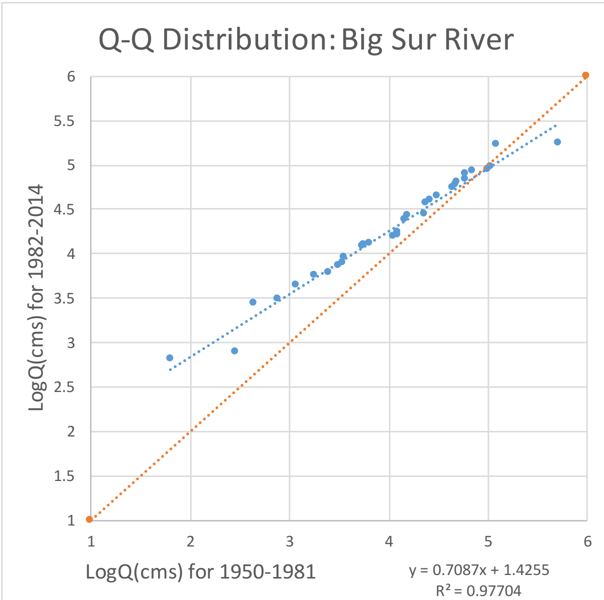
Q-Q Distribution: Big Sur River
LogQ(cms) for 1982-2014
LogQ(cms) for 1950-1981
y = 0.7087x + 1.4255
R² = 0.97704

9F

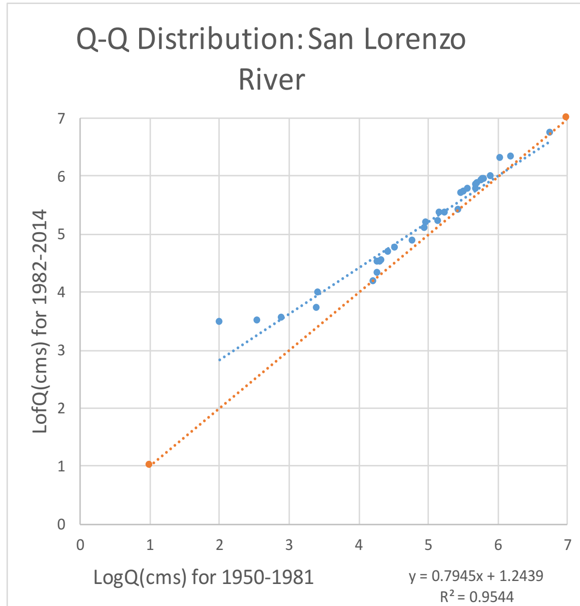
Q-Q Distribution: San Lorenzo River
LofQ(cms) for 1982-2014
LogQ(cms) for 1950-1981
y = 0.7945x + 1.2439
R² = 0.9544

9G

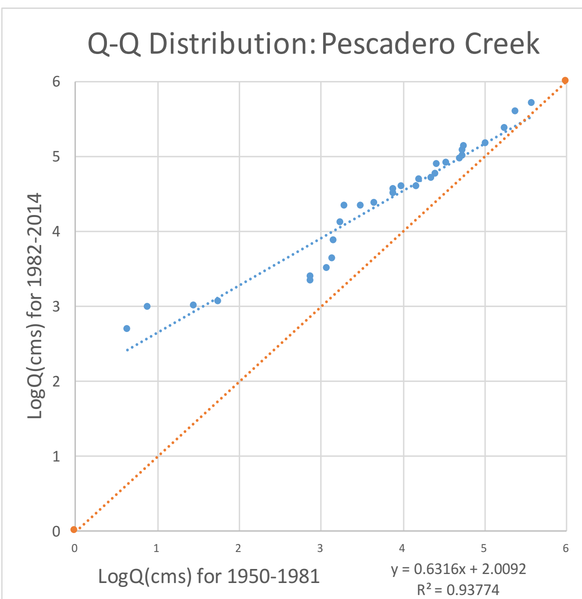
Q-Q Distribution: Pescadero Creek
LogQ(cms) for 1982-2014
LogQ(cms) for 1950-1981
y = 0.6316x + 2.0092
R² = 0.93774

9H

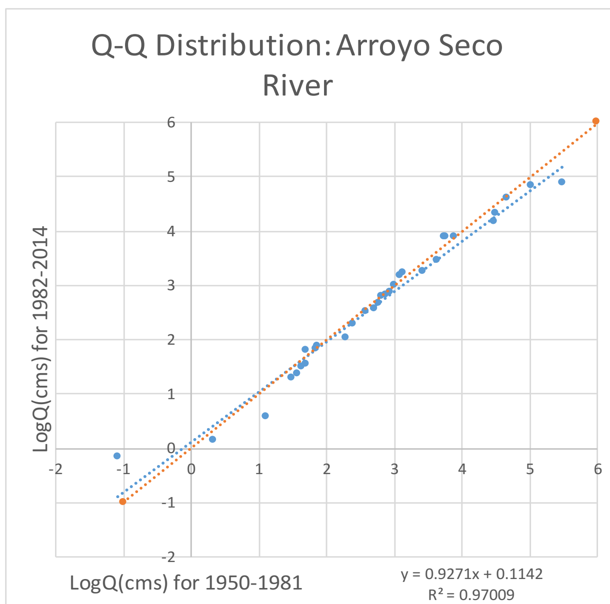
Q-Q Distribution: Arroyo Seco River
LogQ(cms) for 1982-2014
LogQ(cms) for 1950-1981
y = 0.9271x + 0.1142
R² = 0.97009

9I

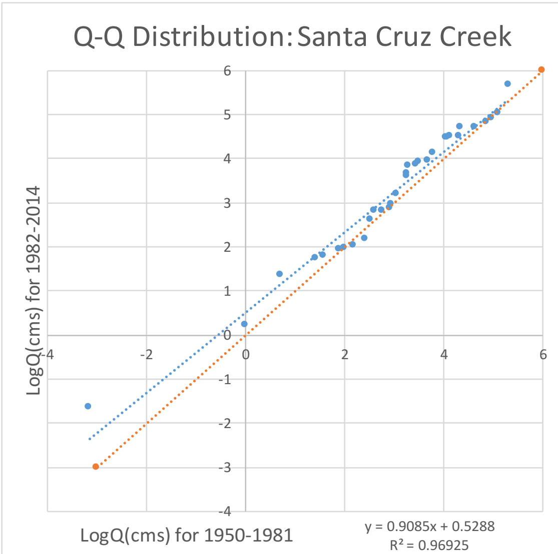

9J

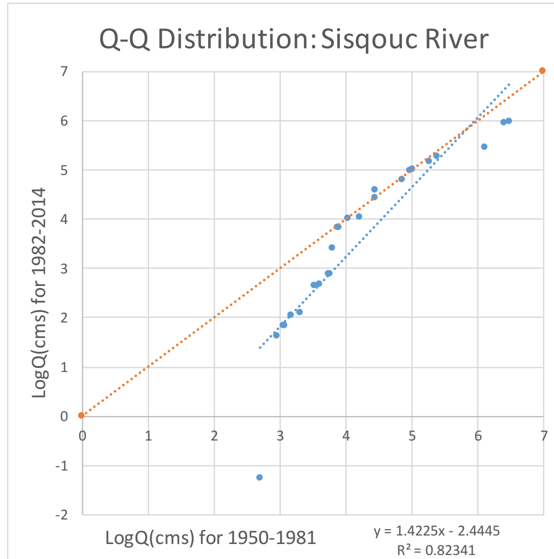

Figure 9A-J shows the Q-Q plot for the logarithmic values of the data for the Southern region. The 1-1 line is depicted as a dashed red line and the trend line for the data represented as a blue dashed line. The linear regression of the trend line and the R^2 are shown in the lower right corner of the graph.